Pergamon

Progress in Nuclear Energy, Vol. 33, No. 1/2, pp. 217–264, 1998

0149–1970/98 $19.00 + 0.00

PII: S0149–1970(97)00100–5

LASER TECHNIQUES APPLIED TO ISOTOPE SEPARATION OF URANIUM

C. Schwab, A. J. Damião, C. A. B. Silveira, J. W. Neri, M. G. Destro, N. A. S. Rodrigues, R. Riva

Instituto de Estudos Avançados, Centro Técnico Aeroespacial
P.O. Box 6044
12.221-970 São José dos Campos - SP
Brazil
e-mail: schwab@ieav.cta.br

A. Mirage

Instituto de Pesquisas Energéticas e Nucleares - IPEN-CNEN
Travessa R, 400 - Cidade Universitária
05508-900 São Paulo SP
Brazil

ABSTRACT

Several countries that utilize nuclear energy around the world are significantly investing in developing laser techniques applied to isotope separation. In Brazil these studies are concentrated in one research institute, the Institute for Advanced Studies (IEAv), and aim toward demonstration of the viability of this process using resources available in this country. In this paper we describe the laser methods for isotope separation, giving an overview of the present status of research and development in this area in other countries and show some results obtained in our laboratories. We focused this report on the atomic route for laser isotope separation, mainly in the areas of laser development and spectroscopy.

KEYWORDS

Laser isotope separation; AVLIS; laser spectroscopy; uranium enrichment; isotope shift; isotope selectivity.

1. INTRODUCTION

The element commonly used as fuel in nuclear reactors is uranium, whose natural composition consists of 99.275% of the ^{238}U isotope, 0.720% of the ^{235}U isotope and 0.005% of the ^{234}U isotope. The large majority of the existing nuclear reactors, on the other hand, requires the uranium to be previously *enriched*, i.e., the contents of the ^{235}U isotope need to be increased to a concentration beyond 3 - 4%. This isotope enrichment is the most difficult stage in the whole process of producing the nuclear fuel. As isotopes of one element are chemically identical, they must be separated by methods based on their physical properties. The traditional methods of uranium enrichment are gaseous diffusion and ultracentrifugation. These processes are based on the small mass differences between the isotopes. The enrichment factors (the ratio between the concentration of the product and the concentration of the natural material) obtained lay between 1.004 (for gaseous diffusion) and 1.3 (for ultracentrifugation), so that, in order to achieve the necessary enrichment for use in reactors, it is necessary to proceed through hundreds of successive stages, the so called *cascades* of enrichment.

In this paper we discuss some aspects of a new technology, proposed in recent years to compete with the traditional ones: the laser methods for isotope separation (LIS). In the next paragraphs we present a summary of the status of research and development (R & D) in this area around the world and briefly describe how our group started to work on this subject. In the following sections we discuss the physical principles of the laser methods and present some results obtained in our laboratories, with emphasis in the areas of laser development and spectroscopy. These experiments have been described previously in a meeting of the Brazilian Nuclear Energy Association (Schwab, 1995).

1.1 Present status of laser isotope separation

During the past twenty years, several countries that utilize nuclear energy around the world have invested significantly in research and development of new technologies for producing enriched uranium. The traditional methods for producing nuclear fuel are probably going to be gradually abandoned, in favor of these new techniques. The main reason for this is the perspective of a drastic reduction in the costs of production of enriched uranium. Table 1 shows a summary of the present status of R & D in uranium isotope enrichment around the world.

The development of new structural materials, such as Al, Ti and other special metal alloys and composites achieved mainly by the aerospace industry, in the last 40 years, have made the ultracentrifugation method to reach its extreme level of efficiency. Nowadays ultracentrifugation and the laser separation methods seem to be the most competitive among the separation processes. The first one is already being used in an industrial scale by URENCO. The second one is, in most of the involved countries, still in a stage of research and development. Nevertheless, recent reports (Dizard and Knapik, 1994; Lewis, 1993) of the *U. S. Enrichment Corp. (USEC)* and of the *U. S. Department of Energy (US-DoE)* concerning the purpose of operating a commercial atomic vapor laser isotope separation (AVLIS) facility

in the very beginning of the next century shall lead to an increase of the investments in other countries to implement similar projects.

Table 1- Research and development in uranium laser isotopic enrichment, updated from Cavalcante (1987).

COUNTRY	DIFFUSION	CENTRIF	CHEMICAL	HELIKON	JET NOZZLE	LASER	PLASMA
S. Africa				A		B	
Argentina	A						
Australia		B				B	
Brazil		A			A[a]*	B	D
Spain	B[b], D						
U.S.A	C	A**	B			A, F	B
France	C	B	A			A	B
Netherlands		C[c]				B	
India**							
Israel						B	
Italy	B	B				B	
Yugoslavia		P_A	P_B			P_B	
Japan	B,B[c]	C	A			B	
Pakistan	P[f]	C,C[e]					
Germany		C[c]			A[a]	B	
China	C	C[e]				B	
Sweden						B	
Switzerland			B			B	
U.K.		C[b]				A	
USSR	C	E					

Stage of R&D	
A -	Pre-industrial
B -	Laboratory/Pilot
C -	Industrial
D-	Research
E -	Lack of information
F -	Technology ready for industrialization
P -	Project
P_A -	Industrial project
P_B -	Laboratory project

Cooperation	
a -	Brazil/Germany
b -	EURODIF
c -	URENCO
d -	Japan/USA
e -	Pakistan/China
f -	Pakistan/Argentina

U.S.A	United States of America
U.K.	United Kingdom
USSR	Former Soviet Union

* Suspended activities
** Agreement with Russia (Unknown method)

The U. S. choice by the AVLIS process was mainly due to economic reasons (Davis et al., 1982). Over and above that, the modular nature of AVLIS allows the installation of smaller plants, which can be easily upgraded according to the fuel demand (Sewell, 1992), while the other processes postulate always large scale plants, due to their smaller separation factors. AVLIS looks, therefore, the most indicated process to substitute the traditional ones in producing enriched uranium. Nevertheless, a successful commercialization of this technology will threaten well established fuel cycle activities. Different specifications of feed material and products and the necessary changes in the interfaces may generate resistance to the deployment of the AVLIS technology from users and from companies in the fuel cycle

activities. In spite of this, several countries proceed with plans and studies on the new laser processes.

1.2 History of the Brazilian laser isotope separation program

The earliest works on AVLIS are generally attributed to the laboratory experiments of Ambartzumian and Letokhov (1972) and to an US patent awarded to Levy and Janes (1973), workers at AVCO Everett Research Laboratory.

In 1972 the USA started the molecular (MLIS) laser isotope separation program in Los Alamos (Jensen et al., 1982) and the atomic (AVLIS) laser separation program in Lawrence Livermore (Davis and Davis, 1977). In this same year Sergio Porto, a Brazilian researcher, was a professor at Caltech and at the University of Southern California, and used to meet ("social meetings") Brazilian students in the USA. They discussed the possibility of developing a similar laser program after their return to Brazil. One of those students, the officer of the Brazilian Air Force José A. A. Amarante formed effectively a laser group as part of what was later called the Brazilian autonomous nuclear program.

In 1974 an agreement between the National Nuclear Energy Commission (CNEN) and the Aerospace Technical Center (CTA), in Brazil, created the isotope separation program. In this same year a research contract between CTA and the State University of Campinas (UNICAMP) was also signed. Some very promising issues related to laser isotope separation in nitrogen and in boron resulted from this cooperation. Although, the real interest of these studies was the uranium enrichment. In this respect the progress was not so quick. After some preliminary experiments in the molecular process at UNICAMP and in the atomic process at the Institute for Atomic Energy (IEA), a new research institute was founded, in the city of São José dos Campos, in the state of São Paulo. Since then the experiments on laser isotope separation have been concentrated in this institute, the Institute for Advanced Studies (IEAv).

2. PHYSICAL PRINCIPLES OF THE LIS METHODS

The physical principles of the laser techniques for uranium isotope separation differ fundamentally from those of the traditional methods. In the case of ultracentrifugation and gaseous diffusion, the separation is based on mass differences between the various isotopes. The fundamental parameter in the laser techniques is the differentiated capacities of different isotopes in absorbing light of particular frequencies.

The various ways of separation by laser differ in how the selective excitation is attained and in how this excitation is transformed into separation. According to this, one can make the distinction between the two processes for laser isotope separation: the molecular and the atomic processes. In the molecular process, the energies of interest are those of the molecular vibrations, which present shifts in the infrared absorption spectra. These isotopic shifts are proportional to the reduced masses of the vibrators. The isotopic shifts, in spite of the fact of being relatively large, are usually (and specially for the heavier elements) hidden by overlappings due to hot bands and rotational structures (Fuss and Kompa, 1981). In such cases the isotopic structures can only be revealed if the molecules are cooled down to about 50 K. In the case of uranium separation, the molecules of UF_6 are diluted in a carrier gas and adiabatically expanded in vacuum, in order to prevent condensation by cooling. UF_6 can then be selectively excited using 16 μm lasers (resonant with the ν_3 vibration at 630 cm^{-1}) and undergo photolysis to UF_5, which is solid and easily separated from the gas phase.

In atoms, the isotopic differences in the absorption spectra are caused by the volume effect of the nucleus and by the nuclear spin of the isotopes. The electronic energy levels present shifts in the visible range of the spectrum, and such shifts allow one of the isotopes to be selectively excited by a monochromatic laser beam. In the case of uranium, the two principal isotopic species differ by 3 atomic mass units in their nuclei. This is a very small difference, if compared to the large nuclear masses.

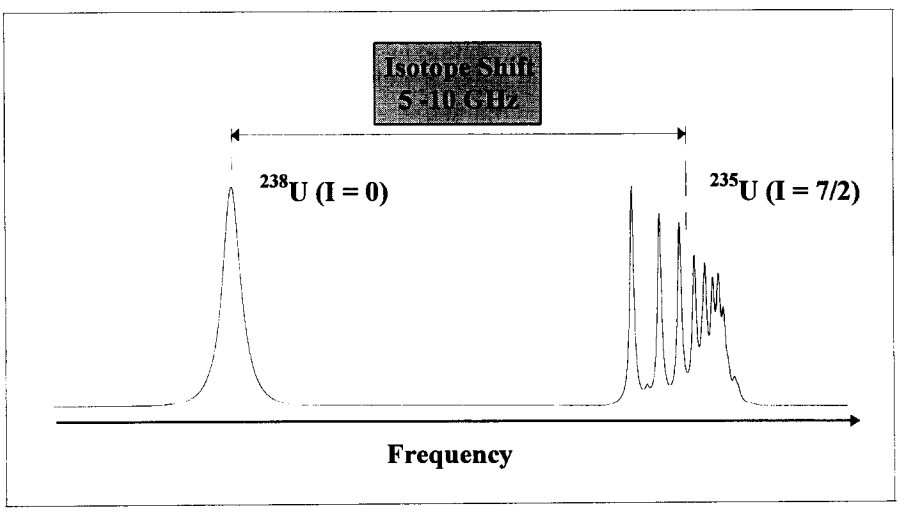

Fig. 1- Appearance of the absorption spectrum of uranium around 600 nm.

The appearance of a spectrum of uranium at wavelengths around 600 nm can be seen in Fig. 1. The scale has been changed between the two absorption lines. Two effects can be observed here: a 5-10 GHz frequency shift and a difference in the line structure. The last one is the hyperfine structure due to the nuclear spin of the 235 isotope. There are actually 21 lines which are here not resolved (Destro, 1993). Thus, if a mixture of these two isotopes is irradiated by a laser beam which has a resonant frequency with the 235 isotope and a sufficiently narrow line, the light of the laser will be preferentially absorbed by this isotope.

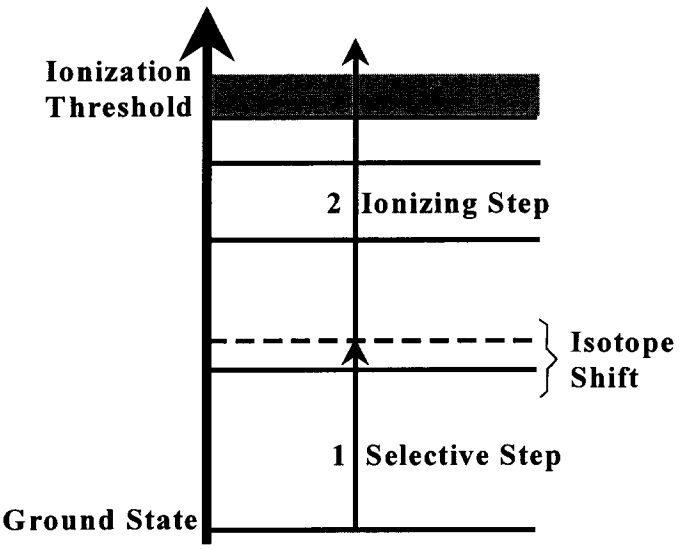

Fig. 2 - Two-photon scheme for selective ionization.

The isotopic separation of uranium by laser and metal vapor (AVLIS) is based on this fact. First, metallic uranium is vaporized by an electron beam. The ^{235}U isotope of this vapor is selectively excited by a laser beam. This selective laser absorption step is represented by line 1 in Fig. 2. In order to be ionized, the atoms must still absorb another photon, so that the energy of the two photons together is greater than the ionization limit (6.18 e V). This corresponds to the transition 2 of Fig. 2. None of these frequencies is resonant with the ^{238}U atoms, which are, therefore, not affected during the process. Actually, this two-photon process is not considered to be the most efficient one. Moreover, the fact that the second ionizing frequency lies in the ultraviolet region of the spectrum would reduce considerably the lifetimes of the dyes used as light sources for the process.

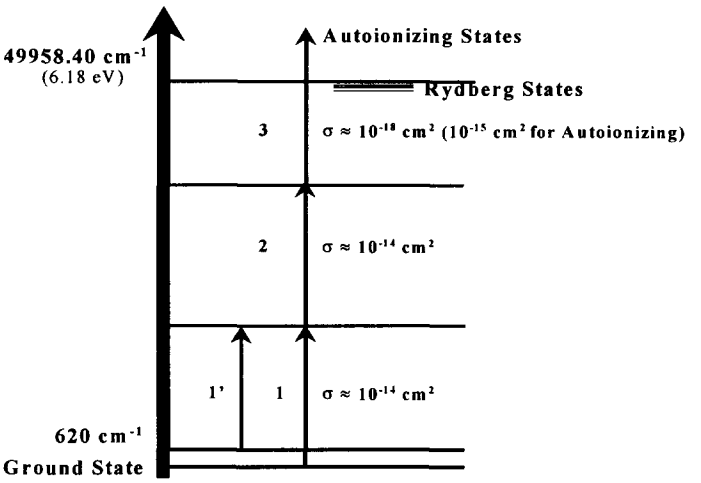

Fig. 3 - Three-photon four-color scheme for uranium photoionization.

Figure 3 shows what seems to be the most efficient way to selectively excite and ionize uranium atoms (Soubbaramayer, 1987). It is a three-photon four-color scheme, where the fourth color is to be used at any practical plant, considering that, in normal conditions of the process, around 30% of the atoms in the vapor are in the first excited state at 620 cm^{-1}.

After the photoionization, the ions can be deflected by electrical and/or magnetic fields and guided up to a collector located in a place not accessible to the neutral ^{238}U atoms, as shown in Fig. 4.

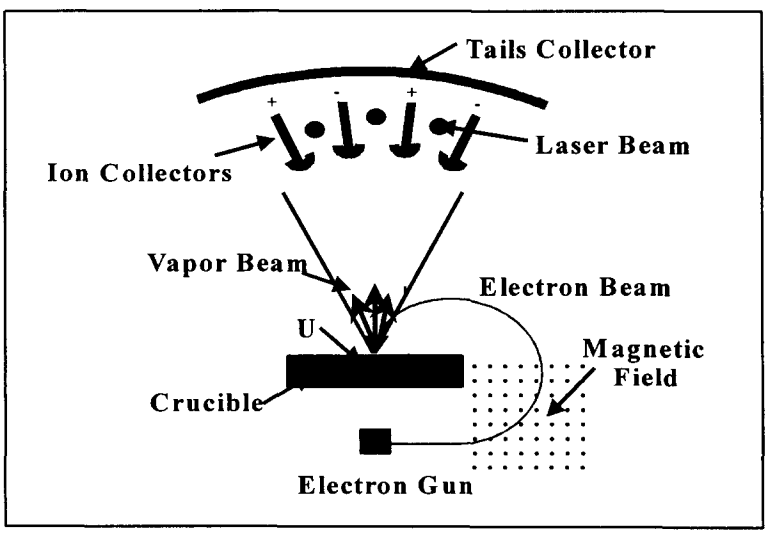

Fig. 4 - Scheme of the evaporation and collection system.

2.1 Some Aspects of the Molecular Process

Photochemical studies are presently being carried out on a variety of compounds and on their decomposition products, in order to obtain a method of deuterium separation with CO_2 lasers. A study on the isotopic exchange between *H* and *D* was initiated with this objective.

Another interesting subject under study at IEAv aiming for isotopic separation by lasers in the molecular process combines the formation of molecular clusters by a gasdynamical process and the inhibition or destruction of these clusters in one of the isotopic variations by means of laser radiation (Airoldi et al., 1988; Sbampato, 1994).

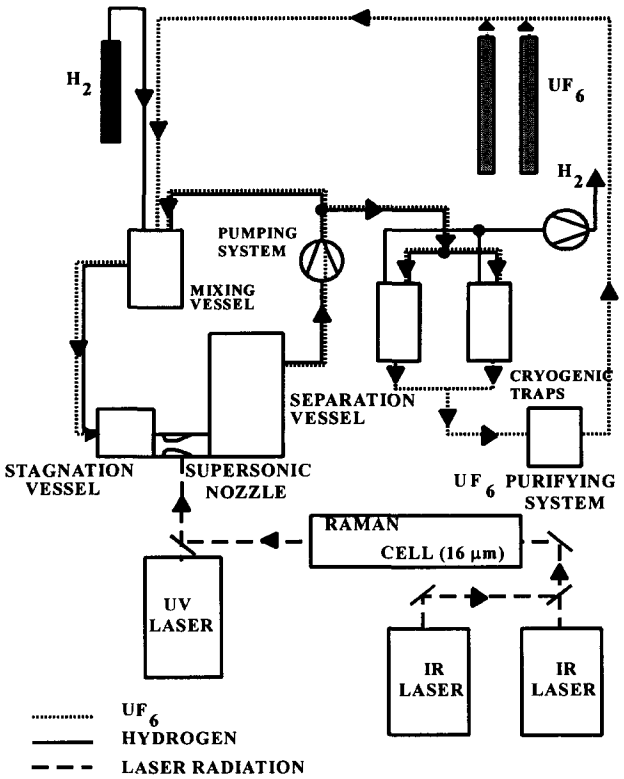

Fig. 5 - Experimental setup for molecular uranium laser isotope separation.

With respect to uranium, Fig. 5 shows the sketch of the experimental apparatus used at our laboratory. UF_6 is expanded together with hydrogen in a supersonic nozzle. The 16 μm radiation is produced by Raman conversion of TEA CO_2 lasers in a multipass para-hydrogen cell. This radiation excites selectively the $^{235}UF_6$ molecules. Photolysis is then performed by UV lasers.

2.2 Some Aspects of the Atomic Process

A basic module used in the AVLIS process is formed by two mechanically independent systems. In what we call the "evaporation systems" occur the processes of atomic vapor generation, interaction between atoms and light, collection of ^{235}U ions, and of depleted uranium. This system includes the electron gun, the vacuum system, product and tails collectors, the crucible with metallic uranium, a mass spectrometer and other probe systems for the vapor and for the generated plasma.

In the "laser system", on the other hand, occurs the production of the necessary radiation for the photoexcitation and photoionization of the selected isotope. It includes basically the copper vapor and dye lasers, the systems of power and tuning control of the lasers and the beam combination and transport optics.

All the processes mentioned above are complex and their understanding offers the many possibilities of selecting and combining parameters that determine the performance of the system.

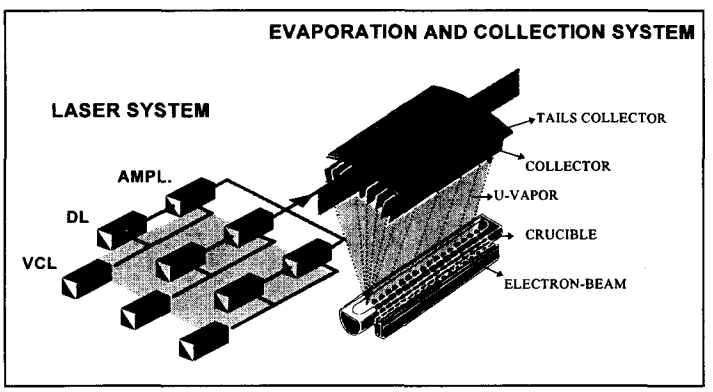

Fig. 6 - AVLIS basic module.

Figure 6 gives an idea of the basic module as described above. This scheme is rather simplified. In an industrial plant uranium must be continuously fed and therefore continuously collected. In a laboratory-scale experiment, such as our experiments, uranium is fed once as an ingot and, after evaporation and photoionization, the product is collected in a cold plate, where the vapor is cooled down to solid state. Then the system is opened and, after crucible and collector replacement, a new run begins. The metallic uranium contained in the crucible is evaporated by an electron beam. The vapor expands upwards in vacuum and is then illuminated by the laser system and selectively ionized. The 235 uranium ions are extracted from the neutral background by means of suitable fields and directed towards the collectors, while the depleted vapor flows to the respective tails collector. These processes occur inside a vacuum chamber that must offer some facilities for system alignment, handling, and cleaning.

Uranium is very corrosive at high temperatures. So, the cathode of the electron-gun must be kept protected from the atomic vapor, otherwise the uranium vapor condensed on the e-beam

gun filament will produce an alloy that degrades quickly its performance. Then the filament should not have a direct view of the crucible surface, and the beam of electrons must be deflected by magnetic mirrors, as shown in Fig. 4 and Fig. 6. The deflecting and the conforming fields must be subjects of careful calculations, specially if one takes into account that, in the case of high power guns, phenomena caused by spatial charges have considerable effects.

The use of electron beam (e-beam) presents some advantages over the Joule heating. First, it reduces the effects of corrosion. In the case of Joule heating, heat is transferred to the crucible, whose interface with the liquid uranium is at high temperatures. With the use of an e-beam the heating is localized on the free surface. The interface between the uranium and the crucible can even be maintained in the solid state. Secondly, the e-beam allows to achieve higher vapor densities in the interaction region and consumes less energy than the Joule heating.

Uranium is vaporized by means of a high energy electron gun. The metal vapor must be confined in a region with a suitable shape, in order to maximize the interaction with the laser beam. This means small cross section and a long length which must be crossed longitudinally by the laser. This effect can be obtained in two different ways: by a linear electron beam or by a point electron beam driven by a fast scanning system. In the first case, the electrons are emitted from a long filament and, after being properly shaped by suitable fields, are guided and focused onto a linear region on the surface of the sample. In the second case a conventional electron gun is used (whose focus is nearly punctual) and then a fast scan is made in one dimension, as shown in Fig. 7. In both cases the vapor is produced in a nearly linear region and expands upwards to the interaction region.

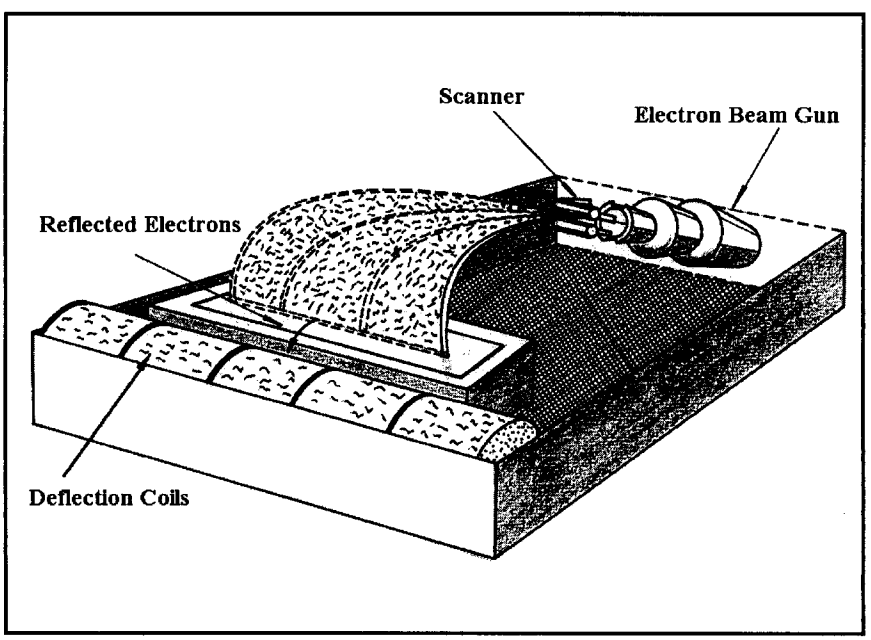

Fig. 7- Fast scanned, point electron gun.

In the interaction region the continuously flowing vapor must be illuminated by high power pulsed lasers. Besides the usual laser properties, such as tunability, high intensity, and coherence, the lasers must possess a high repetition rate in order to illuminate all the atoms in the flux. In order to preserve the selectivity of the excitation, it is also necessary to have a pulse duration smaller than the particle collision time ($\sim 10^{-6}$ s) and smaller than the radiative relaxation time of the intermediate state ($\sim 10^{-7}$ s). The best choice presently is represented by tunable pulsed dye lasers pumped by copper vapor lasers. Copper vapor lasers show efficiency of about 1%, power up to 100 W, and up to 10 kHz repetition rates. These lasers will be described below.

In order to cover all the steps of the process, extensive studies are presently being carried out on subjects such as:
1. Vapor production including electron-beam technology, studies on the uranium-crucible system (corrosion, buoyancy and Marangoni flows) and on the vapor expansion;
2. Photon production involving copper vapor and dye laser technologies, laser spectroscopy, power and tuning control;
3. Uranium spectroscopy aiming the choice of the best channels leading to the stepwise photoionization;
4. Light-atom interaction with emphasis on mathematical modeling using both the rate equations and the Schroedinger equation, taking into account high pulse power, short pulse duration, and the Rabi frequency.
5. Plasma behavior and ion extraction problems.

The photoionization process presents a very high selectivity. It is about 100% in our experiments. Nevertheless, the overall selectivity is degraded in the process of ion extraction and collection, so that the assay of the product mixture lies usually between 5% and 60% of ^{235}U.

The enrichment factor of an isotopic separation process is defined as the relation between the isotopic ratios in the product and in the feed materials ($\alpha = R_P/R_F$) in one stage. In the process we are describing (AVLIS), this quantity lies between 7 and 200. These values are much higher than those reached by each stage of gaseous diffusion ($\alpha = 1.002$) and ultracentrifugation ($\alpha < 1.3$) methods. This fact allows the necessary enrichment of uranium for nuclear reactors in only one stage. Moreover, it allows the production of enriched uranium from materials already depleted by the traditional means ("tails stripping").

3. LASER STUDIES RELATED TO ATOMIC VAPOR ISOTOPE SEPARATION

As previously mentioned, the AVLIS process needs laser systems that can deliver *tunable-in-the-visible* beams, with high peak power at high repetition rates. The natural candidate that fulfills these requirements is the Dye Laser pumped by Copper Vapor Laser (CVL). In this case, both laser systems work in the Master Oscillator Power Amplifier (MOPA) configuration. For laser oscillators, it is generally valid to say that, the higher the output power the more difficult is to control spectral characteristics and beam quality. Spectral characteristics are controlled by dispersive optical components (prisms, diffraction gratings, etalon interferometers, birefringent filters, etc.) placed inside the laser resonator (Demtröder, 1996). The low damage threshold of these components virtually forbids their use in high power systems. So, when tunability and spectral purity at high power are desired, it is recommended to have a low power oscillator, that determines the spectral characteristics of the beam, followed by power amplifiers. This configures a typical MOPA chain and that is the reason why the dye laser, for AVLIS purposes, is designed using this configuration.

Intracavity elements (iris, pin-holes, drilled mirrors etc.) are used also in the case where beam quality is the desired characteristic, and the same argument can be used to recommend a MOPA chain configuration in this case (Siegman, 1986). By good quality beam we mean laser beams with very low divergences and with a smooth transversal intensity distribution. The lowest theoretical limit for the divergence is that due to diffraction. The laser beam that approaches this limit is said to have a "near diffraction limited" divergence.

In the specific case of Copper Vapor Lasers, there are still more arguments for using MOPA configuration. Although there are in the literature references to CVL's with average output power of about 750 W (Knowles et al., 1994), these systems require expensive and/or complex high voltage switches and presents conversion efficiencies (electric into optic power) lower than devices with one tenth of this power. Moreover, high power CVL's require large bore discharge tubes, what generates laser beams with large cross sections and bad quality. This happens because, for the CVL, the small signal gain, a parameter that, together with the saturation intensity, characterizes a laser active medium, concentrates near the tube walls and determines laser beams with doughnut-like transversal intensity distributions, while an ideal laser beam should have an intensity distribution with maximum at the axis and decreasing radially (Siegman, 1986).

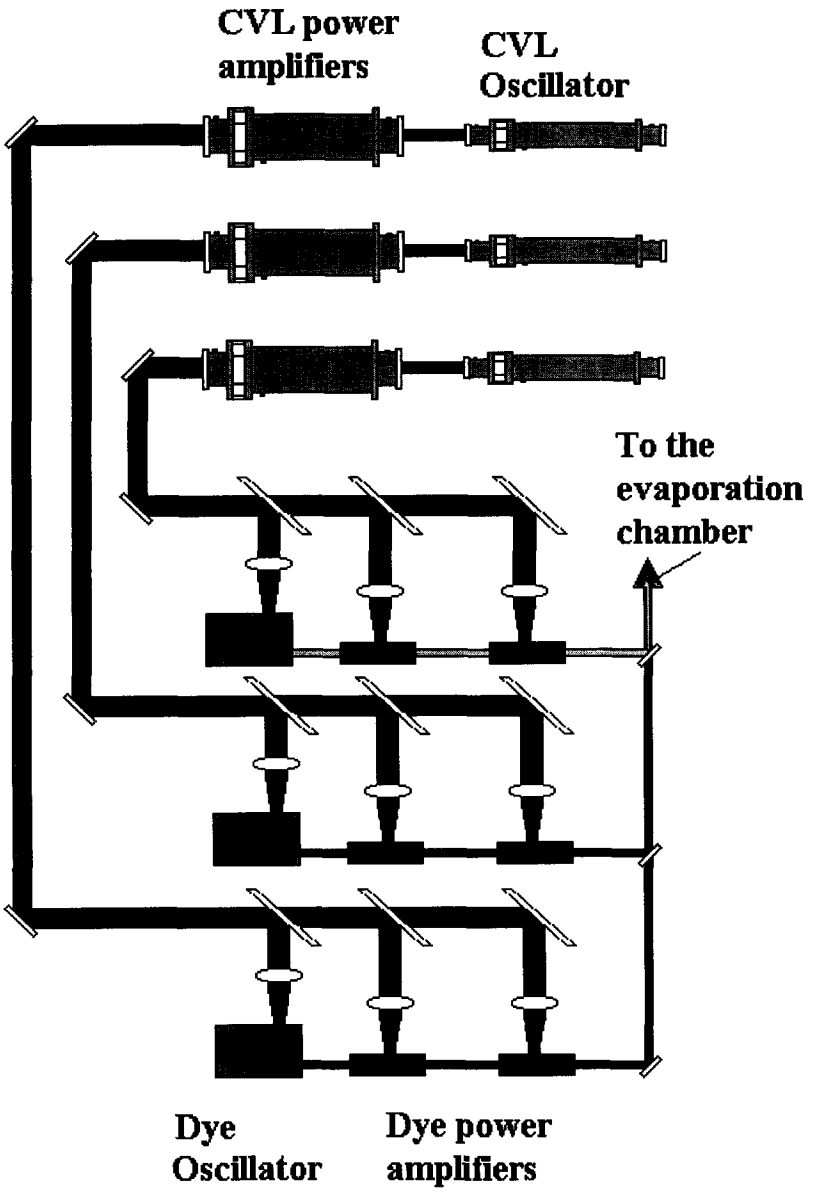

Fig. 8 - Simplified diagram of a hypothetical laser system for AVLIS purposes. The Copper Vapor Laser MOPA chain pumps the Dye Laser MOPA chains that generate the narrowband tunable radiation.

The MOPA configuration can have many different designs. Figure 8 shows a diagram of a hypothetical MOPA chain, constituted by dye lasers pumped by CVL's, that permits the generation of three beams with different frequencies. The CVL oscillators are low power devices that assure good quality beams (near diffraction limit); the amplifiers must raise the

power while keeping the beam quality. The dye oscillators are low power devices that assure narrowband tunable beams; the dye amplifiers must keep the spectral characteristics while raising the beam power. So, the CVL's provide high repetition rate and high peak power pumping for the dye lasers, while these latter ones allow the generation of high power narrowband tunable beams.

The copper vapor laser is a gas laser excited by electric discharge. Its active medium is generated by evaporation of pieces of metallic copper placed inside the laser tube and a buffer gas (Ne or He) is added to sustain the discharge. The same electric discharge that excites the Cu atoms heats the solid copper to about 1500°C to generate Cu vapor. The laser action occurs in two different lines, with $\lambda = 5106$ Å (green) and $\lambda = 5780$ Å (yellow), with pulse width of 30-50 ns and peak power that easily exceeds 10 kW. For both lines it is a typical three level laser with the following kinetics: impact with electrons excites the copper atoms from the ground state to the upper laser level and the transition from the upper to the lower laser level generates the laser radiation. The lower level is metastable and, consequently, only pulsed operation is allowed and the electric discharge excites preferably the upper laser level. Laser action demands population inversion (upper laser level population larger than lower laser level population) (Siegman, 1986), and since the spontaneous transition from the upper laser level to the lower laser level in copper is very fast (has very high rates), the risetime of the electric pulse must be very fast to populate the upper level before a considerable amount of transitions populates the lower laser level. For a good overview on CVL, see the special issue of the Optical Quantum Electronics (Kim, 1991). For a good theoretical discussion about the CVL kinetics, see Kushner (1981).

The CVL development at IEAv started in 1985, with a first prototype of an externally heated copper bromide system that delivered an average power of about 100 mW at a repetition rate of 100 pps. From this system, the work evolved to self heated true CVL's, with maximum average power ranging from 5 W, from a compact air cooled system, to 40 W for a conventional water cooled system. Every CVL presently in normal operation in IEAv has the same basic design for the laser head, as shown in Fig. 9. A high purity alumina tube is surrounded by a thick fibrous alumina thermal insulator and an external Pyrex glass tube assures the vacuum sealing. There is yet an external concentric water jacket for cooling that also provides the coaxial electric feedback to allow short electric pulses, necessary to the CVL operation. The high purity alumina tube is necessary because it supports very high temperature and, yet, since it has high thermal conductivity, it provides a good temperature uniformity in the gain length. The thermal insulation has to be carefully designed for a given desired output power since the CVL has a narrow temperature range of optimum operation (1500 ± 50 °C) and it is self heated, i.e., the input electric power provides at the same time heating and excitation for Cu atoms.

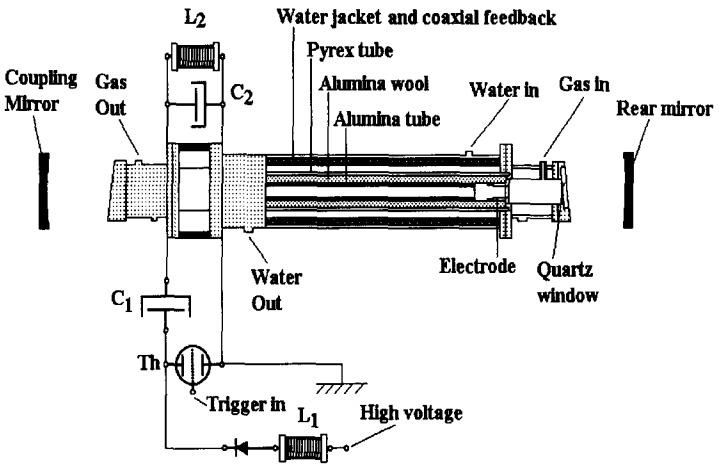

Fig. 9 - Diagram of a conventional CVL head and the excitation electric circuit. L_1 = charging inductance, L_2 = secondary inductance, C_1 = main capacitor, C_2 = peaking capacitor; Th = thyratron.

As we mentioned earlier, the CVL excitation electric circuit must provide high peak current with very fast rise time at high repetition rates. There are many different configurations that can be used for CVL excitation. One of them, very simple and reliable, used in all CVL's at IEAv, is presented in Fig. 9. It is a basic LC inverter circuit where a power supply, with voltage V_0, charges the capacitor $\mathbf{C_1}$ with a voltage $V \approx 2V_0$; when the thyratron **Th** is trigged, there is a negative pulse ($V \approx -2V_0$) and, since the pulse rises very rapidly ($\tau < 10$ ns) due to the peaking capacitor $\mathbf{C_2}$, the charging inductance $\mathbf{L_2}$ presents a high impedance and the energy is preferably transferred to the laser medium. Besides the optimum operation temperature, the electric circuit must be designed to provide the right values for the specific electric field and the peak electric current. This makes the CVL optimization a hard task, since all the relevant parameters are coupled, i.e., the change in one of the relevant parameters implies changes in the others. We built some different CVL's, with different dimensions, thermal insulations, excitation circuits, etc., in order to obtain the necessary experience in CVL design. The three first columns in Table 2 summarize some of the results obtained at IEAv with CVL, using the configuration described above (Schwab et al., 1991; Destro, 1993; Anazawa et al., 1994; Rodrigues et al., 1994). All those lasers are in current use in our facilities, in experiments that range from material cutting, drilling and evaporation to pumping dye lasers for spectroscopy.

CVL development continues in IEAv with the study of a new technology, proposed by Jones et al. (1993a, b), called HyBrID (Hydrogen Bromide In Discharge) copper laser. It consists in adding HBr to the gas buffer; the acid reacts with pieces of copper, in discharge conditions, and CuBr is formed; then, this salt is dissociated due to the impact of electrons, generating the atomic Cu vapor necessary for laser action. The authors referenced above argue that with such a technology the operation temperature can be reduced to as low as 400 °C, the efficiency raised to 3% and, contrary to the conventional CVL, the gain is concentrated at the

laser tube axis, thus propitiating good quality beams. Besides the advantages above mentioned, there is still the fact that the large reduction in operation temperature allows the use of cheaper and not so noble materials for the laser heads.

Table 2 - Summary of CVL Achievements.

Characteristics	Cu5 - Air	Cu10	Cu40	Cu-HBr
Average Power (W)	5	11	38	27
Optimum pulse repetition rate (kHz)	9	9	6	18
Pulse repetition rate range (kHz)	7-13	6-12	5-10	8-20
Green/Yellow ratio (typical)	1.5:1	1.5:1	1.5:1	1.3:1
Pulse energy (mJ)	0.6	1.6	6.5	1.5
Pulse width (ns)	30	40	50	30
Peak power (kW)	20	30	160	50
Beam diameter (mm)	10	18	42	15
Full angle divergence (mrad) - standard cavity - unstable resonator	 6 0.5	 6 0.5	 6 0.5	 N.A.
Runtime on one metal load (hours)	60	200	300	N.A.
Electrical efficiency (%)	0.6	0.92	0.95	1.3
Power consumption (kW)	0.84	1.2	4	2.1
Gas consumption (liter-atm/hr of neon)	1	1	1	N.A.
Cooling	Air cooled	2 liter/min tap water (60 psig)	3 liter/min tap water (60 psig)	1 liter/min tap water (60 psig)

We assembled a test prototype using a 10 W conventional CVL, similar to the one in the second column of Table 2, as a working bench. We used the same excitation and control circuits with changes in the values of capacitors and inductance, the vacuum system was altered to work with two gas cylinders (Ne and HBr) and coal filters were added to the vacuum line, between the laser and the vacuum pump, to prevent damages due to the acid. The original laser head was replaced by one constituted simply by an alumina tube, surrounded by a quartz tube, supported and sealed by water cooled flanges, as shown in Fig. 10. This prototype is not yet completely assessed, but the preliminary results we have obtained are very promising. Some of these results are shown in the last column of Table 2. With this very simple laser head, we have obtained more than twice the output power of a conventional CVL with the same active medium dimensions. The conversion efficiency is almost 50% higher and the prospects are that we can double this figure. These results indicate that the copper vapor laser technology can be improved, in terms of efficiency, compactness and simplicity, making the AVLIS process, for uranium enrichment, even more efficient and simpler than it is nowadays.

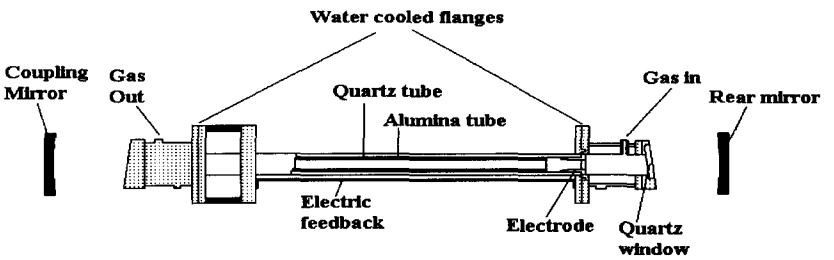

Fig. 10 - Diagram of the Cu-HBr laser head.

The dye laser active medium consists usually of an organic dye diluted in a solvent (ethanol, methanol, water, etc.), optically pumped by flash lamps or other laser (argon, excimer, CVL, etc.). With a set of different dyes, it is possible to obtain continuously tunable laser action from the near infrared to the near ultraviolet, achieving conversion efficiency (pumping power into laser power) above 30% in the middle of the visible range of the spectrum. Besides that, with convenient resonator designs, it is possible to obtain very narrow bandwidth laser beams. All these characteristics make this class of lasers a powerful tool for spectroscopic purposes (Schaefer, 1973; Lago et al., 1989). The dye laser can be assembled in many different configurations, depending on the required characteristics. It can operate from pulsed regime, with pulsewidth of fraction of picoseconds, to continuous wave; in the pulsed regime, it can work from single shot to high repetition pulse rate (kHz for pulsed pump until MHz for modelocking); it can emit in narrow (some MHz) or broadband (tens of GHz), and so on. The choice of the regime of operation determines the design of the pumping scheme, the dye cell and the optical resonator. In the case of AVLIS purposes, the dye laser must operate in pulsed regime, at repetition rates of about 5-20 kHz, with output peak power in the range of tens of kilowatts. A diagram of the dye oscillator developed at IEAv, to be used in AVLIS experiments, is shown in Fig. 11. It is basically a folded grazing incidence dye laser (Lago et al., 1989). The diffraction grating allows the selection of radiation wavelength and its resolution depends on the angle of the incident light beam, i.e., the bandwidth of the feedbacked radiation is narrower the smaller is the angle between the incident beam and the grating surface. The tuning mirror, in front of the diffraction grating, allows the laser tuning, feedbacking radiation with a certain wavelength depending on the angle it faces the diffraction grating. The spherical folding mirror is used to compensate the astigmatism introduced by the grating. This configuration is quite versatile since, simply by adjusting the incident angle of the laser beam over the diffraction grating (tuning the grating around its own axis), it is possible to vary the laser bandwidth and efficiency, and simply by adjusting the turning angle of the tuning mirror it is possible to tune the laser within the dye bandwidth. The dye cell and the flowing system are designed to allow about ten changes of the active volume (volume that is illuminated by the pumping laser) between two consecutive pulses, to allow efficient heat exchange and to prevent dye depletion. The dye depletion happens because part of the excited dye molecules returns to the ground state, and part decays to a metastable state (triplet); from this metastable state the molecule can be dissociated by absorbing light from the next pumping pulse. With the device diagrammed in Fig. 11, using Rhodamine 6G in methanol, we

obtained bandwidths between 500 MHz and 10 GHz, conversion efficiencies between 8% and 25%, and maximum output power of 200 mW. Since in the range of the visible the uranium isotope shift and the ^{235}U absorption bandwidth (broadened by the hyperfine structure) lie around 5-10 GHz, this type of dye oscillator is quite convenient for AVLIS purposes.

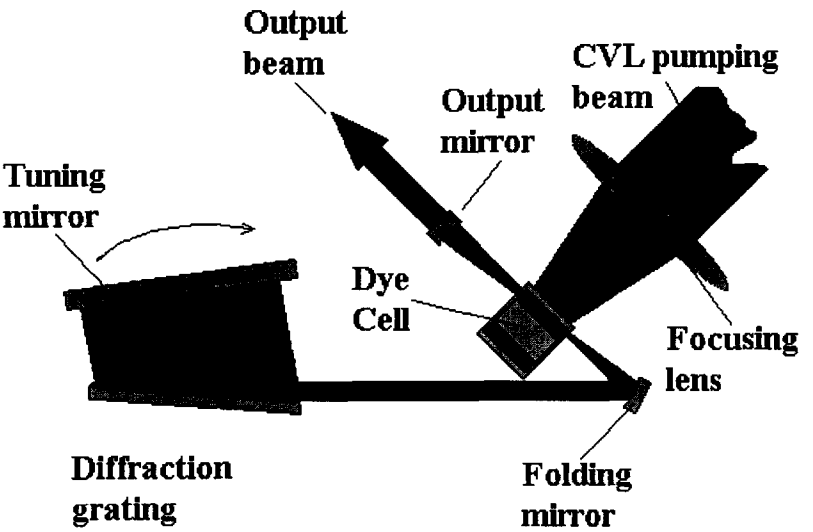

Fig. 11 - Diagram of the dye laser oscillator used in IEAv.

The dye amplifier is simply a dye cell, similar to the one represented in Fig. 11, pumped by the CVL. The beam coming from the dye oscillator crosses the dye cell. More than 1 W of average power was obtained with two stages of amplification, in the peak of the Rhodamine 6G emission, while keeping the oscillator spectral characteristics. In spite of its simplicity, this amplifier can have conversion efficiencies easily above 30% (Destro and Neri, 1992).

4. LASER SPECTROSCOPY FOR ISOTOPE SEPARATION

The spectrum of atomic uranium is extremely complex. Over 92000 known emission lines have been compiled (Carlson et al, 1976; Corliss, 1976; Blaise and Radziemski, 1976; Janes et al., 1976; Solarz et al, 1976; Coste et al., 1982). These lines arise from transitions between levels belonging to numerous electron configurations whose terms show considerable mixing. Roughly 460 odd and 1240 even parity levels have been determined. The uranium atom has 92 electrons but only 86 are in closed electronic shells and the 6 remainder electrons are in valence shells. Thus, the ground state belongs to the (Rn) $5f^3 6d7s^2$, where Rn is the radon atom. In LS coupling approach this level is approximately represented by the $^5L_6^o$ term.

As we have seen, the principle of the laser isotope separation process is based on the isotope shift. This shift occurs because the ^{235}U and ^{238}U nuclei have slightly different radii. The ^{235}U nucleus is smaller so that the nuclear potential felt by the electrons in this lighter isotope is stronger than that in the heavier one. Consequently, each state of ^{235}U is more tightly bound than the corresponding state in ^{238}U. In fact, the absolute binding energies are less important for the laser isotope separation process than the transition energies, and one is usually interested in the isotope shifts of transition. On the other hand, when the spectrum of each one of the odd isotopes of an element is examined in detail, a residual structure is found, which is known as the hyperfine structure. In 1924, Pauli suggested that this was due to a magnetic moment associated with an intrinsic nuclear spin angular momentum. The interaction of the magnetic moment of the nucleus with the magnetic field produced by the valence electrons causes a small splitting of the energy levels of an atom and provides the largest contribution to the observed hyperfine structure (Corney, 1977). Although isotope shifts are very small in uranium (5 to 10 GHz around $\lambda \approx 6000$ Å), they have the same order as the hyperfine structures, and several publications (Gerstenkorn et al., 1973; Böhm, 1977; Böhm et al., 1978; Greenland, 1990; Barbieri et al., 1990; Destro et al., 1992; Destro, 1993) have shown a perfect spectroscopic discrimination between the isotopes.

Different routes can be used to obtain selective, resonant photoionization. The most studied routes using three-step laser photoionization are shown in Fig. 12. There are basically two ways to achieve photoionization after the selective photoexcitation: (i) direct, non-resonant absorption from a highly excited atomic level to the continuum or (ii) resonant transition to an autoionization state of the excited atom. Autoionization states are bound atomic states whose energy levels relative to the outer valence electrons lie above the ionization limit. Usually, above the ionization limit, there are no discrete states and the absorption spectrum is continuum. Nevertheless, for complex atoms like uranium it is observed, slightly above the ionization limit, the presence of discrete states superposed to a continuum of states. Some of these discrete states tend spontaneously towards ionization in a very short time (10^{-11} s) and are called autoionizing states. For uranium, experiments have shown that the absorption cross sections are about: (i) 10^{-14} cm^2 for resonant excitation, (ii) 10^{-17} to 10^{-18} cm^2 for direct ionization and (iii) 10^{-15} cm^2 from autoionizing states (Soubbaramayer, 1987). On the other hand, highly excited states close to first limit of ionization (Rydberg states) are easily ionized by either: (i) applying a pulsed electric field or (ii) using an additional infrared radiation or (iii) collisions with other particle or with the walls of the container. Every uranium photoionization obtained from Rydberg states or from autoionizing states require more than two intermediate resonant excitations.

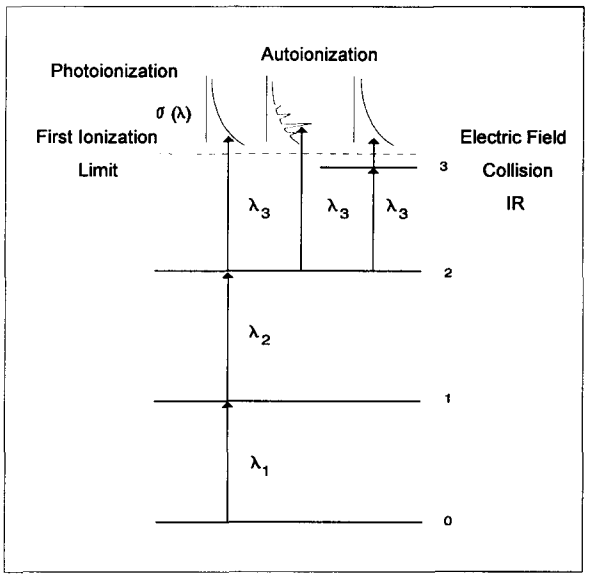

Fig. 12 - Different routes can be used to obtain resonant photoionization.

Although the uranium spectrum has been widely studied and several spectroscopic tables are available (Carlson et al., 1976; Corliss, 1976; Blaise and Radziemski, 1976; Janes et al, 1976; Solarz et al., 1976; Coste et al., 1982), there is a huge lack of information related to both the used techniques and to the great strategic significance of accurate information about laser isotope separation. Most of the data have been obtained by conventional spectroscopy. We present below some results obtained in our laboratories with conventional and intermodulated laser optogalvanic spectroscopy and with laser multistep photoionization spectroscopy.

4.1 Optogalvanic Spectroscopy

The resonant absorption of radiation by atoms or molecules, that occurs in a self-sustained discharge, changes its electrical properties. This change is observed as an increase or decrease in the conductivity of the discharge and is known as *the optogalvanic effect* (Barbieri et al., 1990). This effect has been shown to be a powerful and inexpensive technique for investigation of atomic and molecular species, and is particularly useful in the spectroscopy of refractory elements, like uranium. Many extensive theoretical and experimental works have been published in recent years showing results obtained from optogalvanic spectroscopy (Gagné et al., 1979a, b; Lawler et al., 1979; Erez et al., 1979; Shuker et al., 1983; Broglia et al., 1983, 1985; Engleman et al, 1987; Destro, 1993).

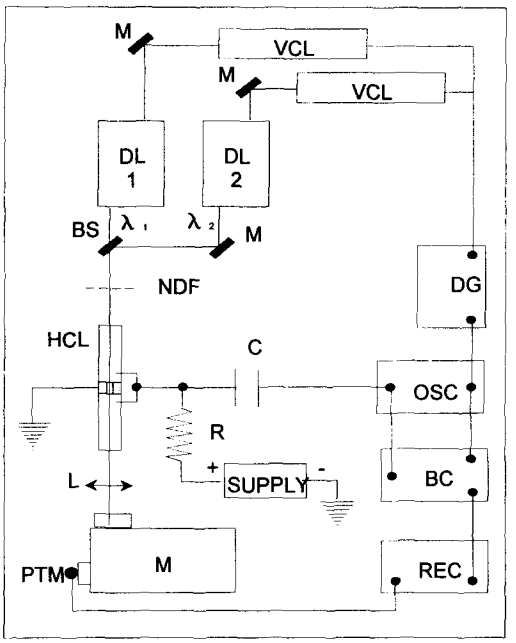

Fig. 13 - Optogalvanic spectroscopy experimental setup. CVL = Copper Vapor Laser; DL = Dye Laser; BS = Beam Splitter; M = Mirror; NDF = Neutral Density Filter; HCL = Hollow Cathode Lamp; DG = Delay Generator; C = Capacitor; R = Resistor; OSC = Oscilloscope; BC = Boxcar Averager; PMT = Photomultipler; M = Monochromator; Rec = Recorder.

Figure 13 shows the experimental setup we used to obtain two photon absorption assignments with conventional optogalvanic spectroscopy in a similar way as Broglia (1983). In these experiments we used a natural uranium hollow cathode lamp (HCL) with 2.6 mbar argon gas as buffer, made in the Institute for Energy and Nuclear Research (IPEN), in São Paulo. The 15 mA and 318 Vdc electrical discharge are supplied by a stabilized voltage source through a 1.8 kΩ resistor, and the optogalvanic signal (OGS) is coupled in a Tektronix Oscilloscope model R7630 with a Tektronix Programmable Digitizer model 7D20 (OSC) and in a Boxcar Averager EG&G Princeton Applied Research model 162 (BC) by a 1.2 nF isolator capacitor. The OGS was recorded by a HP 7046B- XY plotter from a signal f(t) obtained from the boxcar averager. The dye lasers used here were Molectron Tunable Dye Lasers Model DL14P (DL) pumped by Copper Vapor Lasers (CVL). This laser system delivers about 100 mW average power, at 5 kHz rate pulse frequency with 25 ns pulsewidth and about 700 MHz linewidth. We also used a half meter Spex Monochromator to obtain rough spectra calibrations. Figure 14 shows some of the spectra we have obtained and the results are summarized in Fig. 15.

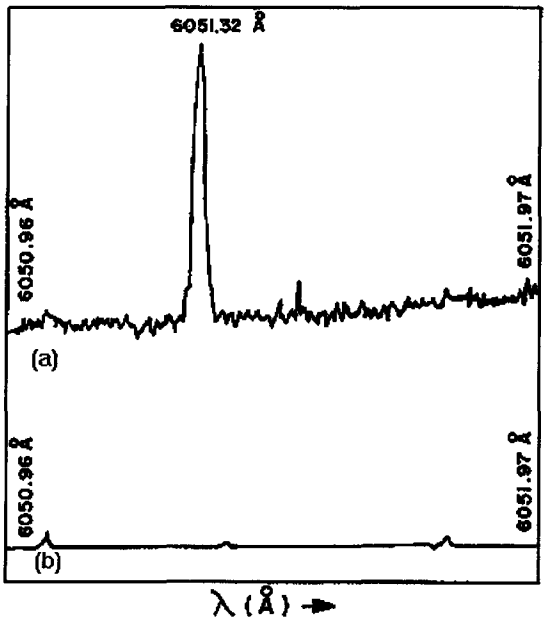

Fig. 14 - a) Sequential two-photon absorption spectrum obtained with optogalvanic spectroscopy. DL1 was kept fixed on the first transition, $^5L_6^o - {}^7M_7$, at 5915.39 Å, and DL2 was swept around the second transition, $^7M_7 - {}^7L_6^o$, at 6051.32 Å. **b)** Sweeping DL2 wavelength with DL1 off.

The same setup shown in Fig. 13 was used to obtain the lifetimes of uranium excited levels, the U-Ar collisional impact parameter as well as superelastic relaxation rates. The only change we made was the replacement of the Tektronix Oscilloscope model R7630 and the Tektronix Programmable Digitizer model 7D20 (OSC) by a Tektronix 500 MHz Digitizing Oscilloscope model TDS-744A. Figure 16 shows the excited levels used to measure these parameters.

After tuning the dye lasers resonantly with the transitions shown in Fig. 16, as pointed out above, we recorded the total two photon optogalvanic signal against the delay between the two dye laser pulses to a given discharge current and voltage of hollow cathode lamp. The plot of the optogalvanic signal against the delay between the two dye laser pulses shows two distinct regions: one where it is dominated by the laser pulse shape, and the other dominated by transition decay, as we can see in Fig. 17.

The effective lifetime of level 1, in our case the $^7M_7$ uranium level, is related to the hollow cathode discharge current by (Svelto, 1989; Neri et al., 1995)

$$\frac{1}{\tau_{eff}} \approx \frac{1}{\tau} + \alpha + \beta I \quad ,$$

where τ is the radiative lifetime of the level, the coefficient α is the U-Ar collisional relaxation rate and β is the electron collision coefficient. Hence, if the radiative lifetime is known and we measure the effective lifetime against the hollow cathode discharge current, we can obtain the α and β coefficients as shown in Fig. 18.

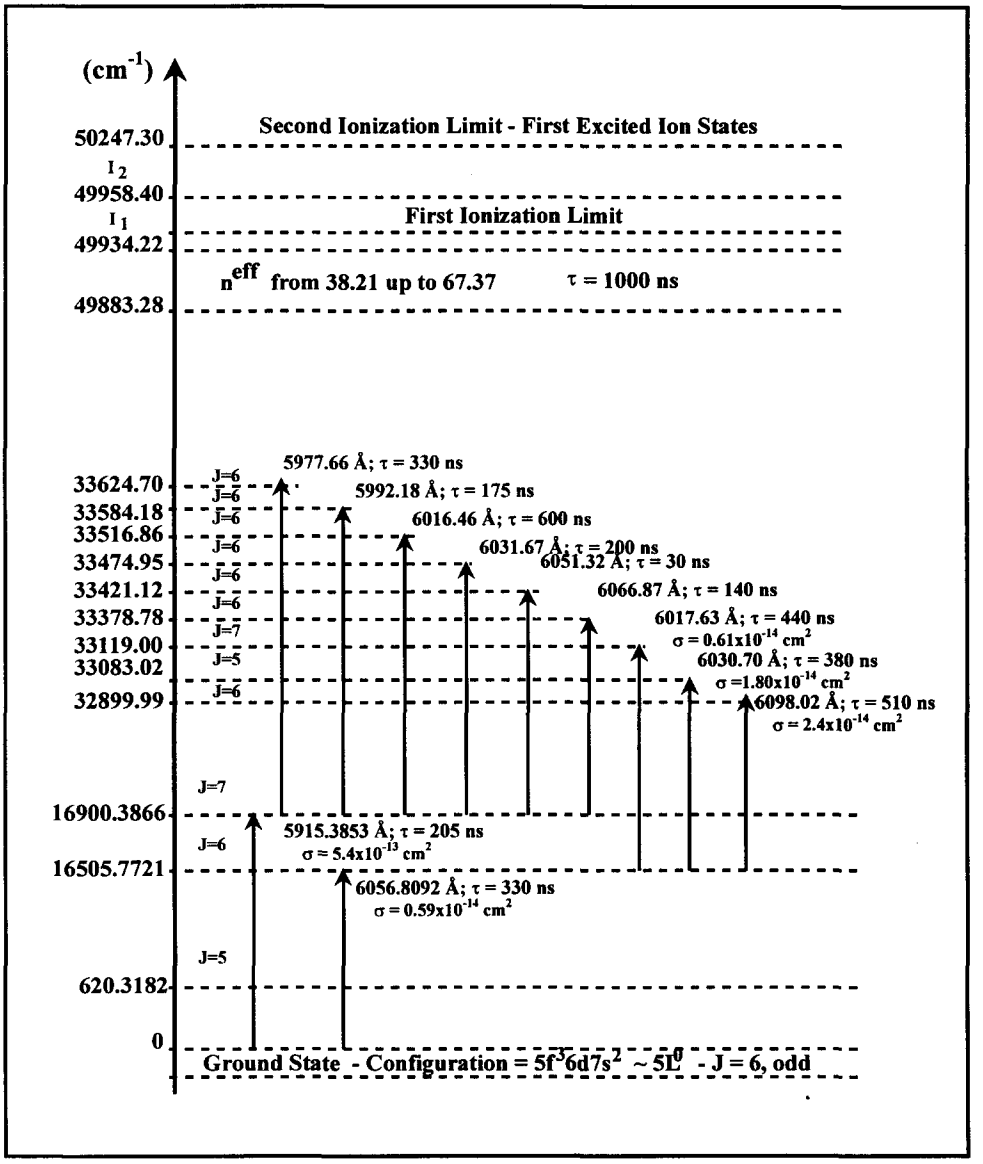

Fig. 15 - Observed two-photon absorptions. The lifetime and absorption cross section values are obtained from the literature (Carlson et al., 1976; Corliss and Bozman, 1962; Miron et al., 1979; Chen and Borzileri, 1981; Destro et al., 1991).

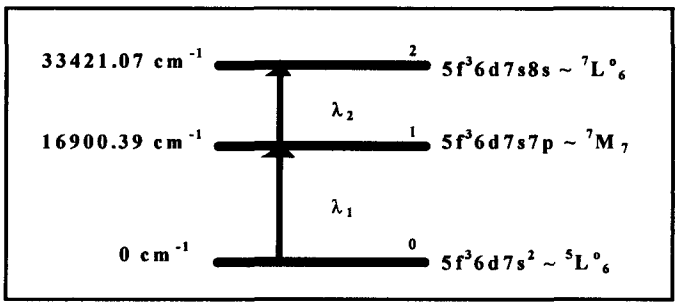

Fig. 16 - Diagram of the used excited levels.

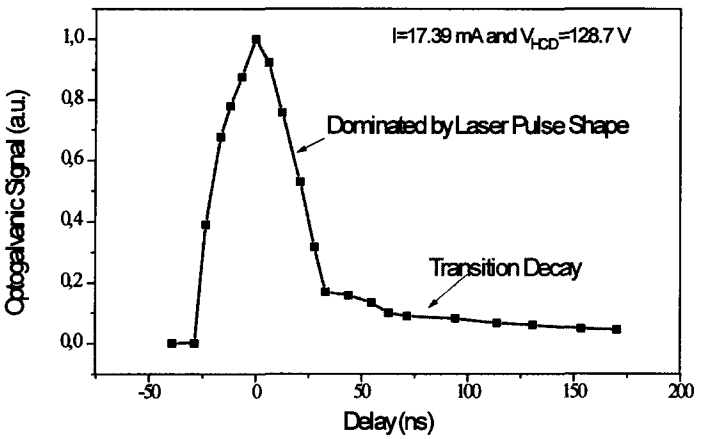

Fig. 17 - Optogalvanic signal against delay between the two dye laser pulses.

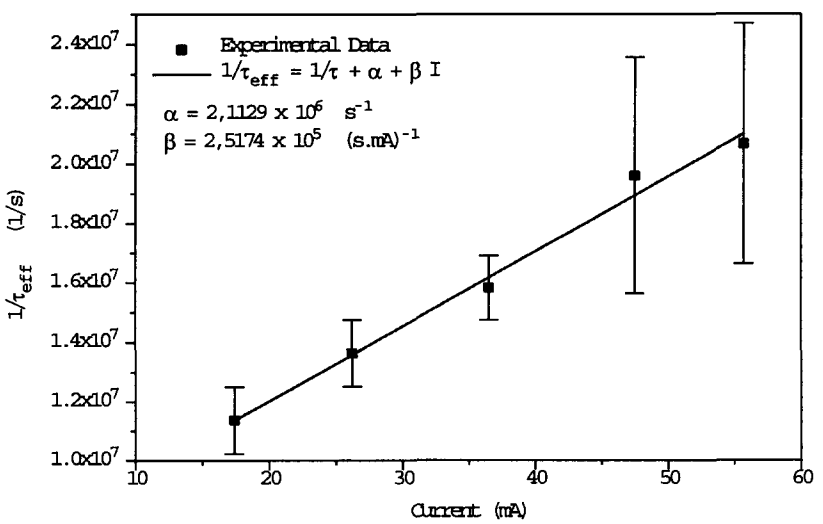

Fig. 18 - Effective lifetime against hollow cathode discharge current.

4.2 Intermodulated Optogalvanic Spectroscopy

The first sub-Doppler spectroscopic observation using optogalvanic detection was made by Johnston (Barbiere et al., 1990). He obtained the characteristic Lamb dip at the center of the resonance due to the optogalvanic effect in atoms with a zero-velocity component along the light direction, when he recorded the profile of the line through a He-Ne discharge that was irradiated by a dye laser and the transmitted beam was reflected by a mirror back into the discharge. In order to avoid the background characteristic on Lamb dip measurements, it was necessary to develop a technique sensitive only to the saturated signal due to the atoms absorbing photons from both beams, that is, the signal to be observed must arise directly from nonlinear mechanisms. This effect can be obtained by using the intermodulation technique (Barbieri et al., 1990). This sub-Doppler Technique was introduced by Sorem and Schawlow (1972) for fluorescence spectroscopy and then applied by Lawler et al. (1979) to optogalvanic spectroscopy. The basic mechanism of this technique can be understood with the help of Fig. 19.

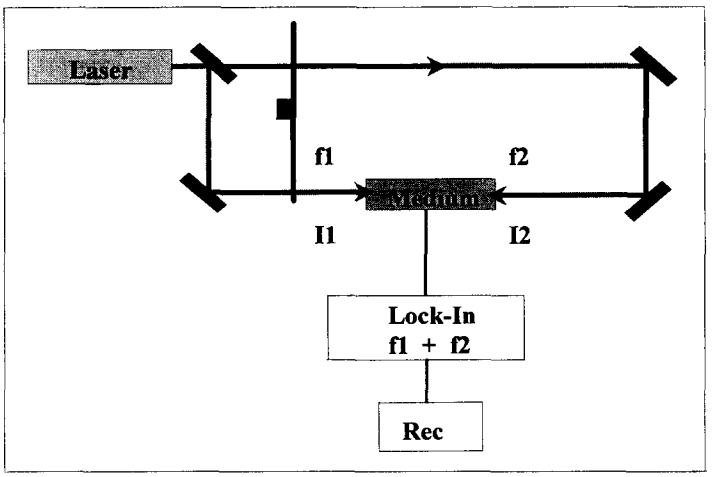

Fig. 19 - Typical diagram used in intermodulated spectroscopy.

In intermodulated optogalvanic spectroscopy (IMOGS) the laser beam, from a continuous dye laser, is split into two components of roughly equal intensities (I1 and I2). One beam is mechanically chopped at a frequency f1 and sent through the discharge. The other beam is chopped at a different frequency f2 and sent through the discharge in the opposite direction. As the two beams propagate in opposite directions, they interact with different velocity groups of atoms under the Doppler profile of a given transition. When the laser is tuned within one homogeneous width around the line center, the two beams interact with the same group of atoms. Nonlinearities caused by the two beams acting to saturate the same transition then give rise to a Doppler-free optogalvanic signal at the sum or at the difference of the modulation frequencies ($f1 \pm f2$). The sum frequency is conveniently detected with a lock-in amplifier (Lawler et al., 1979).

Using this technique and the experimental setup shown in Fig. 20 we were able to solve the hyperfine structure for the $^5L_6^\circ - {}^7M_7$ uranium transition and to obtain the magnetic splitting factor A_j, the nuclear quadrupole coupling constant B_j, experimental spacing values between the hyperfine structure components A, B, C, D, F, G and H as well as the isotope shift for this transitions in a good agreement with the values found in the literature (Gerstenkorn et al., 1973; Böhm, 1978).

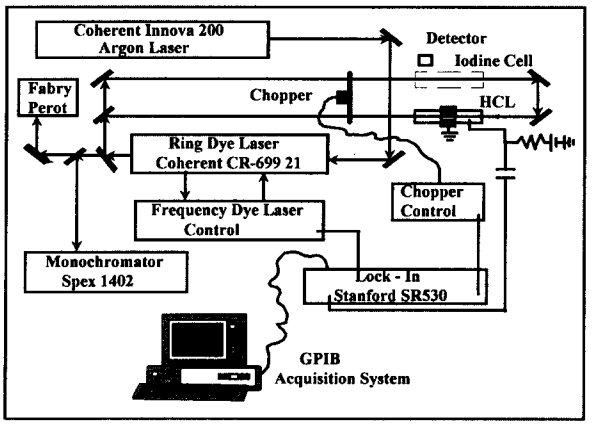

Fig. 20 - Experimental setup for intermodulated spectroscopy.

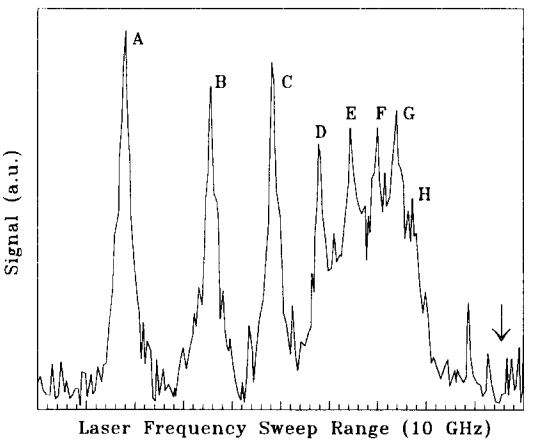

Fig. 21 - Hyperfine structure for the $^5L_6^\circ - {}^7M_7$ transition to ^{235}U obtained from intermodulated optogalvanic spectroscopy.

Figure 21 shows the hyperfine structure for the $^5L_6^\circ - {}^7M_7$ transition of ^{235}U obtained from intermodulated optogalvanic spectroscopy using the experimental setup shown in Fig. 20. The arrow in Fig. 21 indicates the Iodine line transition located at 16900.8228 cm^{-1} that was used

as reference line and calibration for our measurements. The whole sweep of the laser frequency was 10 GHz. From several experimental spacing values measured between the hyperfine structure components and following the steps of Gerstenkorn et al. (1973), we were able to solve also the hyperfine structure for the $^5L_6^o - {}^7M_7$ transition of ^{235}U in a lamp with natural uranium. Tables 3-5 summarize the results obtained and compare them with values found in the literature. Figure 22 shows the theoretical profile of the ^{235}U hyperfine structure for the $^5L_6^o - {}^7M_7$ transition obtained from theoretical values of each component intensity and from the experimentally measured spacing between the components of the hyperfine structure to calculate A_j and B_j values (Destro et al., 1992; Destro, 1993). Comparing Fig. 21 with Fig. 22 we can see a good agreement between the experimental and theoretical profiles of the ^{235}U hyperfine structure for the $^5L_6^o - {}^7M_7$ transition.

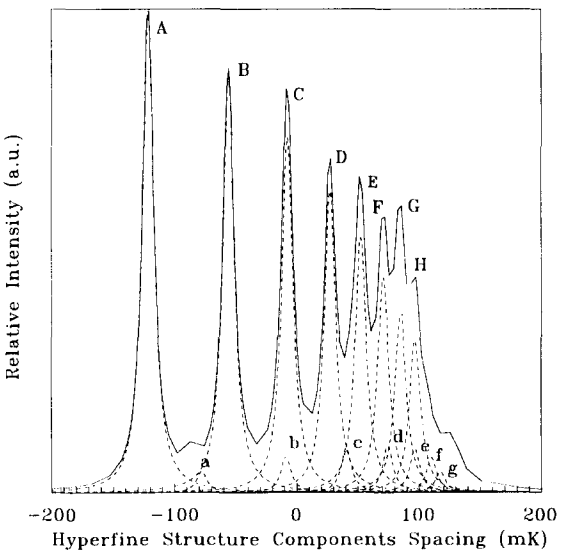

Fig. 22 - Theoretical profile of ^{235}U hyperfine structure for the $^5L_6^o - {}^7M_7$ transition obtained from theoretical values of each component intensity and from the experimentally measured spacing between the components of the hyperfine structure to obtain A_j and B_j values. The solid curve is the hyperfine structure resultant from contributions of each hyperfine component (dashed curves) for this transition.

Table 3 - Magnetic splitting factor, A_j, and the nuclear quadrupole coupling constant, B_j.

Constants	Our Work	Gerstenkorn et al. (1973)	Böhm (1978)
A_6 [mK]*	-2.04 ± 0.03	-2.08 ± 0.03	-1.96 ± 0.03
B_6 [mK]*	133 ± 10	138.5 ± 1	136.9 ± 0.8
A_7 [mK]*	-5.73 ± 0.07	-5.73 ± 0.05	-5.64 ± 0.05
B_7 [mK]*	88 ± 12	89.5 ± 1	86.42 ± 1.7

*1 mK = 10^{-3} cm^{-1}

Table 4 - Spacing between the principal A, B,..., H components of ^{235}U hyperfine structure for the $^5L_6^o - {}^7M_7$ transition.

	Spacing among components [GHz]					
	Our Work		Gerstenkorn et al. (1973)		Böhm (1978)	
Components	Measured	Calculated	Measured	Calculated	Measured	Calculated
A – B	1.74	1.70	1.76	1.76	1.77	1.77
B – C	1.28	1.29	1.29	1.29	1.28	1.30
C – D	0.95	0.95	0.98	0.94	0.94	0.94
D – E	0.63	0.70	0.68	0.68	0.67	0.68
E – F	0.59	0.53	–	0.50	0.52	0.50
F – G	0.36	0.42	–	0.39	0.37	0.38
G – H	0.33	0.35	–	0.33	0.34	0.33
A – H	5.89	5.97	–	5.90	5.90	5.91

Table 5 - Isotope shift between the ^{238}U line and the center of gravity of the ^{235}U components.

	Our Work		Gerstenkorn et al. (1973)		Böhm (1978)	
	mK	GHz	mK	GHz	mK	GHz
Isotope shift	279 ± 4	8.4 ± 0.1	282 ± 2	8.45 ± 0.06	280 ± 2	8.40 ± 0.06

4.3 Multistep Photoionization

Most of the ionization spectroscopy related to AVLIS process performed at IEAv/CTA was accomplished with the setup diagrammed in Fig. 23. Each tunable dye laser MOPA chain, composed by an oscillator and two amplifiers, is pumped by two copper vapor lasers. The beams, after combined in beam splitters, are sent to the furnace and to the reference hollow cathode lamp, so that the experiments can be done either in the atomic vapor generated in the furnace or in the hollow cathode lamp.

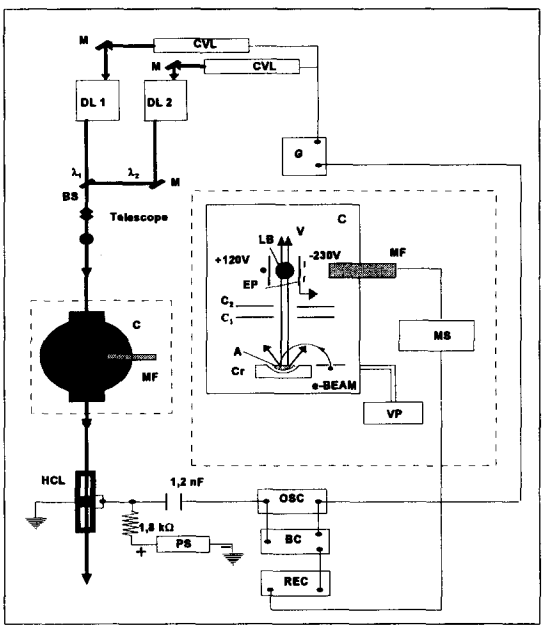

Fig. 23 - Experimental setup. CVL = copper vapor laser MOPA chain; DL = dye laser MOPA chain; BS = Beam splitter; MF = mass filter; MS = mass spectrometer; Cr = crucible; HCL = hollow cathode lamp; V = metal vapor ; LB = laser beams; EP = extraction plates; C = vacuum chamber; PS = power supply; C_1 and C_2 = thermal ions collectors and collimator slits; A = metal target; OSC = oscilloscope; BC = boxcar averager; REC = xy recorder.

4.3.1 Photoionization Experiments in a Furnace

Although the two-frequency scheme is far from the ideal one for AVLIS, we performed three-photon, two-frequency photoionization experiments with the setup shown in Fig. 23, with some interesting results (Destro, 1993; Rodrigues et al., 1994). Figure 24 shows the simultaneously registered optogalvanic two-photon absorption spectrum and ^{238}U photoionization spectrum. These spectra were obtained by scanning the dye laser DL1 of Fig. 23 around the frequency of maximum optogalvanic signal value (the first absorption step in Fig. 16), just after both dye lasers had been tuned for the two-photon sequential absorption,

shown in Fig. 16. The photonionization spectrum was registered in the mass spectrometer recorder, with the mass filter adjusted for the ^{238}U mass and kept fixed during the laser scanning. The optogalvanic spectrum showed two peaks. The peak which coincides with the maximum of the photonionization spectrum was attributed to direct two-photon transitions to the excited level at 33801 cm^{-1} (Destro, 1993; Broglia et al., 1983; Rodrigues et al., 1994). Figure 25 shows the possible mechanisms for absorption of these two wavelengths.

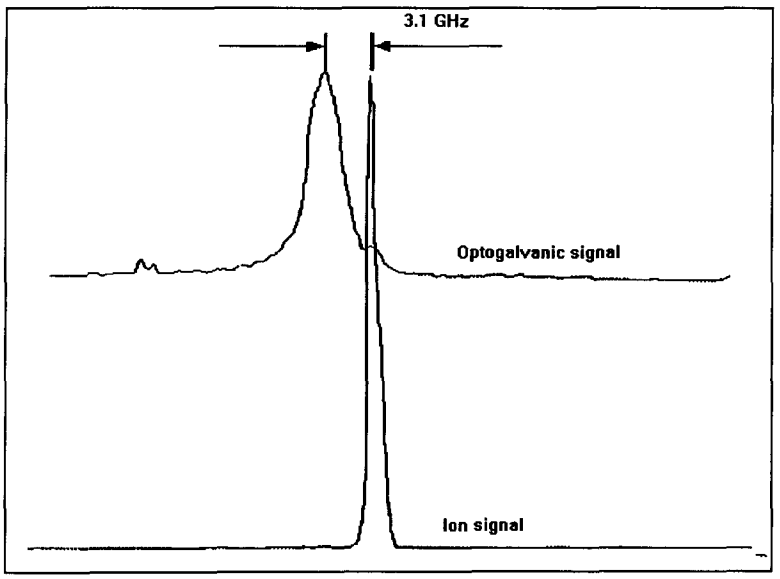

Fig. 24 - Optogalvanic and photoionization signals, for two wavelengths excitation ($\lambda_1 \approx 5915$ Å, $\lambda_2 = 6051$Å). DL1 wavelength is scanned near the single-photon resonance. The ion signal spectrum is understood as being due to two-photon direct absorption of λ_1 followed by an ionizing sequential absorption at λ_1 or λ_2.

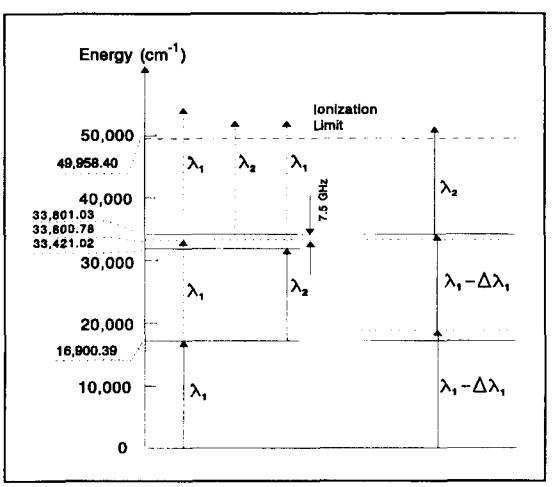

Fig. 25 - Diagram of the possible mechanisms for uranium photoionization, using two-frequency, three-photon absorption with $\lambda_1 \approx 5915$ Å and $\lambda_2 \approx 6051$ Å. The left side indicates the situation when λ_1 is coincident with the linear, single-photon absorption peak and the right side indicates the situation where λ_1 is detuned 3.1 GHz, as indicated in Fig. 24.

Following the same procedure, we selectively ionized the ^{235}U. This was done with the appropriate shift (~ 8.4 GHz) in the first frequency (λ_1), to compensate the isotope shift. Figure 26 shows a typical result obtained from these experiments.

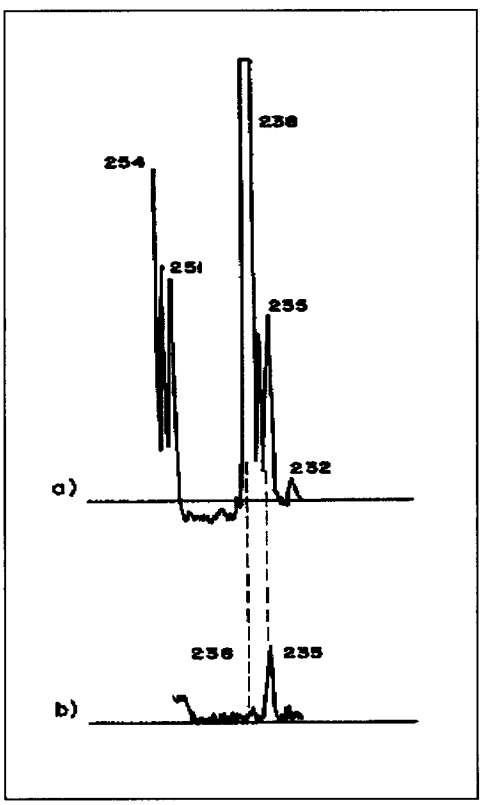

Fig. 26 - Uranium mass spectra. (a) with ions obtained from an e-beam; (b) with ^{235}U ions selectively obtained from laser photoionization.

4.3.2 Experiments in Hollow Cathode Pulsed Discharge

The hollow cathode lamp has been used not only in single photon, but also in multi-photon absorption spectroscopy, although, in this latter application, the buffer gas and the electric current have deleterious effects. Collisions with electrons and with the buffer gas can conceal transitions departing from highly excited states, or induce decays departing from excited states. In general, this only allows up to two-photon absorption detection in the range of the visible. Therefore, the optogalvanic spectroscopy in hollow cathodes is inconvenient for

multi-step photoionization spectroscopy. The effect of collisions with electrons can be reduced if one eliminates the electric discharge effects in the measurements. Gagné and collaborators (Gagné et al., 1979b) showed that, in a pulsed lamp with hollow cathode made of uranium and using Ar as buffer gas, it is possible to have uranium vapor with a density of about 10^{13} cm^{-3}, for more than one millisecond after the discharge is turned off. Babin and Gagné (1986) obtained metal vapor without the undesired electric discharge effects by using a hollow cathode lamp with the buffer gas flowing through an orifice in the cathode, such that the metal vapor is dragged outside the discharge region. They observed that the fluorescence profile of the atomic beam decreased in amplitude and increased in width, becoming blurred with the buffer gas (Ar) pressure rise, indicating a *"probable cloud formation in the output orifice"*. The threshold pressure to observe this effect was about 0.5 torr.

We have performed some experiments with a setup developed to allow photoionization spectroscopy studies in a pulsed uranium hollow cathode lamp. The uranium vapor was generated in the lamp, which was driven by an electric circuit that pulsed the discharge and allowed electric current measurements in the afterglow. To assess such setup, uranium ions were produced in the afterglow by two dye lasers, using the same two-photon photoionization scheme shown in Fig. 16.

The experimental setup is diagrammed in Fig. 27. It consists of a hollow cathode lamp operating in pulsed regime, with a secondary electric circuit that allows electric current measurements during the period in which the electric discharge is off. The lamp cathode is made of metallic uranium, with a 3 mm diameter and 9 mm deep cylindrical hole; a drilled mica disk prevents the discharge in the front surface of the cathode; the lamp is filled with 2.5 torr of argon as gas buffer and sealed with a quartz optical window. The electric circuit has two different parts: the first one (S_1, R_1) assures the pulsed electric discharge and the second one (S_2, R_2) allows ion current measurements.

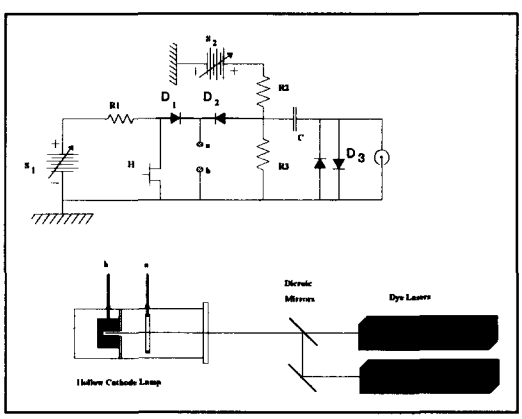

Fig. 27: Experimental setup and electric circuit. The electric circuit values and components characteristics are: Rl = 2 kΩ, R2 = 1 MΩ, R3 = 10 MΩ, Sl (0-4OOV), S2 (0-40OV), H (IRF 730), Dl and D2 (SK4F1/01), coupling capacitor (1.8 nF), clipping diodes (1N4007).

The lasers were pulsed at a rate of 5 kHz. The results obtained with these experiments can be summarized in Fig. 28. The observed electric signal had two contributions: the first one was a distorted sequence of square pulses, with an offset due to the bias voltage, and the second one was attributed to the contribution of ion current. Figure 28 shows the measured electric signal in the afterglow period, where one can see the peaks due to photoionization. Those peaks have been considered as due to photoionization because: (i) they only appeared when the laser beams illuminated the discharge and it was a resonant effect, vanishing with laser detuning; (ii) they did not appear when there was no discharge in the hollow cathode lamp, leading to the conclusion that they are due to the presence of uranium vapor, and not to the Ar buffer gas or to a wall effect contribution (laser ablation, for instance); and (iii) they did not appear without the bias voltage, and the amplitude of the peaks did not vary considerably with the bias voltage, from 6 V up to 40 V, leading to the conclusion that the signal was due to electric charges generated by other agent than the bias electric field.

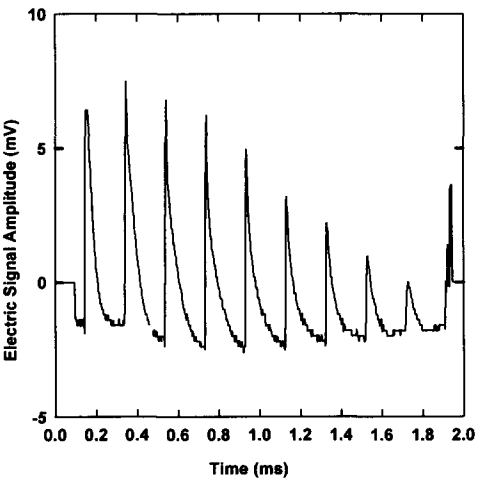

Fig. 28: Typical electric signal in the afterglow period, showing 9 peaks due to photoionization.

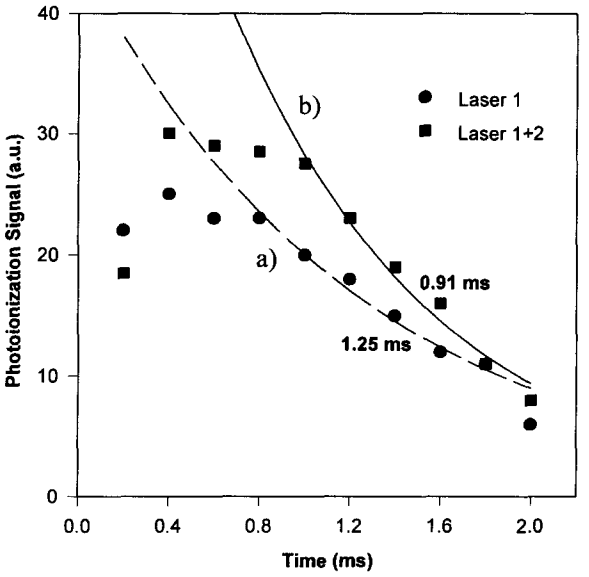

Fig. 29: Photoionization signal time evolution in the afterglow. The symbols indicate the peak value of every photoionization signal, the lines indicate the exponentials fitted to the last 6 experimental points.

Figure 29 shows the photoionization signal time evolution in the afterglow for: a) hollow cathode lamp illuminated only by DL 1 and b) by DL 1 and DL 2 simultaneously. This time-dependent behavior (that corresponds to the time evolution of the ground state uranium vapor density) is similar to that one observed by Gagné et al. (1979a) for the absorption in a pulsed uranium hollow cathode lamp with Ar gas buffer. Fig. 30 shows that the amplitude of the peaks does not vary considerably with the bias voltage, from 6 V up to 40 V.

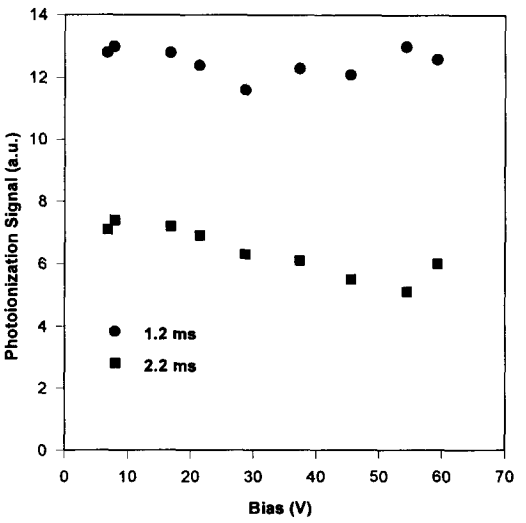

Fig. 30: Photoionization vanishing time versus power supply bias voltage.

With this system, it was observed that it is possible to have uranium vapor for about 1 ms after the discharge is turned off, which is very convenient for our purposes. The long life of the vapor was attributed to clusters formation, which is deleterious, because it decreases the cross sections and it broadens the spectral profile. Some indirect evidences of clusters formation were obtained with the experiments (Neri et al., 1996). The experimental results allowed to estimate a photoionization of about 17% of the ground state uranium vapor.

5. METAL VAPOR PRODUCTION AND ION EXTRACTION

One of the main technological problem of the AVLIS process is the generation of metallic uranium vapor. Due to the intrinsic characteristics of the process, this vapor must be dense and contain only neutral uranium atoms in a very directional beam. High densities are necessary since large amounts of enriched uranium at high production rates are desired; charge neutrality is necessary, otherwise all ions in the laser-vapor interaction region will be attracted to the collectors, decreasing the selectivity obtained with the lasers; and the vapor beam must be directional because, making the laser beams perpendicular to the vapor beam, Doppler spectral broadening can be avoided. In addition, these three aspects are dependent on each other. The goal of this section is to present the problems related to the vapor generation for AVLIS purposes and to comment how these interdependencies are and how these factors affect the selectivity of the collection process. We also present some analyses we have performed at IEAv related to uranium vapor generation.

As far as high production rates are concerned, the higher the vapor density, the faster is the process. However, there is an upper limit for this parameter that must be considered. If the vapor is excessively dense, there will be collisional effects that can destroy the selectivity obtained with the lasers. First of all, one can mention the charge transfer, where an ionized ^{235}U atom, colliding with an neutral ^{238}U atom, captures an electron, being neutralized and generating an ionized ^{238}U atom (Grossman and Shepp, 1991). Moreover, the photoionization selectivity can also decrease, due to collisional spectral broadening, with a consequent decreasing of the peak of the absorption cross section and loss of spectral selectivity.

A neutral vapor is highly desirable since the original fraction of ^{235}U in the vapor is rather low (0.7%). A few percent of ^{238}U ions can be very deleterious for the selectivity of the overall process, because both the original ions and the photoions will be collected together by the electromagnetic fields. However, the usual processes to generate metal vapor intrinsically produce a considerably large amount of ions by thermal excitation. Moreover, when the vapor is produced by e-beams, there is yet the interaction between electrons of the e-gun and uranium atoms, producing excited and ionized uranium. Therefore, special attention must be taken in order to assure that only a neutral vapor reaches the region where the metal atoms will interact with the laser beams. To decrease the amount of ions coming from the vapor generation region, a pair of electrodes is added to extract the ions produced during the vapor generation process, before they reach the vapor-laser interaction region. This primary-ions collector can decrease considerably the amount of ions that achieve the laser-vapor interaction region, but can not completely eliminate them. There are also other ion sources like thermal ionization and ionization by electron impact. The higher the metal surface temperature, the higher is the ion density and, while evaporating the metal with e-beam, the higher the e-gun power, the higher is the ion density.

The directionality of the vapor beam can be achieved by working at very high temperatures. After the vapor is produced it propagates outwards the surface of the molten metal, with a density distribution that can be described by

$$\phi = \phi_0 \left(1 - \frac{\phi_{Is}}{\phi_0} \right) \cos^n(\alpha) + \phi_{Is} \quad ,$$

where α is the angle between the flow direction and the normal to the metal surface, n is a constant that increases with the evaporation rate, ϕ_0 is the vapor density at $\alpha = 0$ and ϕ_{ls} is the isotropic portion of the vapor stream (Schiller et al., 1982). The equation above indicates that the higher is the evaporation rate, the more collimated is the vapor beam. High evaporation rates, on the other hand, mean high surface temperatures. However, there is some upper limit for the metal surface temperature basically due to three reasons: a) Higher metal surface temperature means higher vapor density and, as we pointed out earlier, there is an upper limit for vapor density; b) Higher temperature means higher thermal ionization rate and consequently higher primary ion density; and c) There is yet an increase of contaminant density due to chemical reactions between uranium and crucible material, that we shall discuss further. Therefore, there are compromises among collimation, collisional effects and contamination that must be carefully considered.

Metal vapor is produced in a vacuum chamber by heating a metal source until its vapor pressure is high enough to produce a beam with the desired density and collimation. The vapor generation from solid metal can be made either by Joule or by electron-beam heating. In the first case a resistor heats a crucible that contains the metal. This method is the simplest one, but has a serious drawback, as far as uranium is concerned: liquid uranium is highly reactive and the higher is the temperature, the more reactive it becomes. In the case of Joule heating, the highest uranium temperature occurs in the interface with the crucible, that is seriously attacked by the liquid metal. This chemical attack not only destroys the crucible, but also contaminates the metal vapor. If the crucible is made of an oxide, for example, uranium reacts with the oxygen and, since the uranium oxide has a vapor pressure higher than the metallic uranium at the same temperature, most of the vapor produced can be oxide instead of pure metallic uranium. The use of electron gun to heat the uranium reduces the chemical reaction with the crucible (although doesn't eliminate it completely) because, since the heat flows through the open surface, the uranium temperature has the lowest value in the interface with the crucible. Nevertheless, also with the use of electron-beams, very often the temperature on the interface is still high enough to produce serious damage to the crucible. If the purpose of the vapor is spectroscopy, the presence of contaminants is not so serious because they produce only an almost constant background around the resonant absorption frequencies. However, if the idea is to collect enriched uranium, the ionization of the contaminants decreases the overall efficiency of the process. The contamination by crucible material impairs the AVLIS processes in two ways: a) The increase of contaminants tends to decreasing the metal vapor density and b) Some contaminants are easily multi-step photoionized by radiation in the visible, decreasing the spectral selectivity. The reduction of contaminants is a subject that can be faced in many different fronts:

- Study of crucible materials not so heavily attacked by liquid uranium. In the literature there are many references about crucible materials that are adequate to working with uranium, but for temperatures limited to about 1200 °C, since these works focus on the metallurgy of uranium (Harrington and Ruehle, 1959; Burke et al., 1976; Wilkinson, 1962). The temperature necessary to evaporate uranium efficiently lies about 2000°C and, at this level, most of those materials are seriously damaged by uranium chemical attack.

- Reduction of the temperature on the crucible interface (large uranium block, efficient cooling, and so on). This alternative solution to decreasing the uranium attack is to cool the crucible such that the uranium is solid on the interface between uranium and the crucible wall.

As far as AVLIS process is concerned, an efficient crucible cooling means an inefficient evaporation process, since most of the delivered power is spent in heating water. Since one of the goals that AVLIS must strike is low power consumption, this solution is virtually forbidden.

- Decrease of liquid uranium convection (also related to power loss). Another solution to reduce the chemical attack to the crucible walls is to dump the convective currents in the molten metal. In an ideal liquid metal with null convective flow, the rate of chemical reaction with the container walls is much smaller than in a liquid with convection. This solution has much in common with another problem, the power loss and how the e-beam power is distributed in the process. Much effort has been made based on this idea and some interesting results have come out thereby. Blumenfeld and Soubbaramayer (1994) calculated that, for the evaporation of cerium with a 5 kW axis symmetric electron gun, about 71% of the total power is lost in convection, while only 1.7 % is used in evaporation. So, a considerable gain in efficiency can be obtained if the convective flow can be dumped. One way to do so is to apply a magnetic field on the molten material that, according to the authors, can increase the evaporation rate by a factor between 2 and 3. Another possible way to decrease the convective flow is to use sweeping axial e-beams. Since the AVLIS demands long interaction paths between lasers beams and vapor, the metal vapor is generated in a narrow and long area that is, very often, heated by a linear e-beam. If this *linear* region is heated by a sweeping axial e-beam, instead of by a linear one, the evaporation efficiency in the optimum sweeping frequency can be increased by a factor between 10 and 35 for the same electron gun power (Couairon and Soubbaramayer, 1992). This can be understood as follows: A sweeping e-beam with a spot diameter d and a linear velocity v illuminates an area $\pi d^2/4$ during a period of time of about $\tau = d/v$. The diffusion length corresponding to this illumination time is $l = \sqrt{\alpha\tau}$, where α is the thermal diffusivity. In this case, the evaporation process occurs as if a pulsed e-beam had illuminated the target with a pulse length τ and an energy of $P\times\tau$, where P is the e-beam power. If l is much smaller than the target dimensions, τ is much smaller than the time the beam takes to illuminate the same area again and the absorbed energy is enough to generate vapor, the molten pool size and the power loss due to convection are considerably reduced.

- Increase in the vapor generation at lower temperatures with the use of special alloys. There are strong evidences that for certain uranium alloys it is possible to obtain the same evaporation rate at lower temperatures than in the case of pure uranium. This can reduce the population of contaminants by reducing the temperature of operation and by reducing the uranium concentration, thus reducing the rate of the crucible chemical attack by the liquid uranium.

A numerical model was developed to describe the uranium vapor expansion, charged particles behavior and ion collection problems. The neutral and ionized uranium were described as particles whereas electrons were described as a fluid in a bidimensional frame. The program furnishes the evolution in time of the velocity distribution function of neutrals and ions, for a jet of neutral particles that penetrates a region where there is some applied electric field (initial condition for the model) and where the particles are ionized. Although this model had been developed specifically to study collection and plasma problems, it furnished an interesting result related to evaporation: at an uranium density of about 10^{13} cm^{-3}, the collisions rate has the same magnitude as the rate the ionized atoms are extracted by the

electric field, i.e., the necessary time to extract one ion from the metal vapor is comparable to the average time between two consecutive collisions. So, at this uranium density, collisional effects begin to become relevant in the process, as we stated in the beginning of this section.

We are also performing some experiments with uranium evaporation using a 20 kW home made axial-beam e-gun, installed in a vacuum chamber, in order to model the vapor expansion as a function of the temperature. Two complementary diagnostic methods are being used to monitor the uranium vapor expansion. The experimental setup for uranium evaporation experiments is shown in Fig. 31. Eighteen aluminum plates are kept at the same distance to the e-beam spot, making different angles with the normal to the heated surface, as indicated in the figure. The temperature on the uranium evaporating surface was measured with an optic pyrometer and the uranium mass deposited on the aluminum plates was measured both by: weighing before and after the evaporation; and by alpha spectroscopy of the ^{238}U. By fitting the density distribution equation given above to the experimental data, we obtained the exponent n varying from 1.2 to 7, with the temperature varying from 1350 °C to 2300 °C. The second diagnostic using the same setup is the absorption spectroscopy, using dye lasers, that we are still working on. Comparing the results obtained with the two methods, we intend to describe experimentally the expansion of uranium vapor generated by an axial continuous beam and to calculate the vapor expansion behavior for linear and sweeping axial beams.

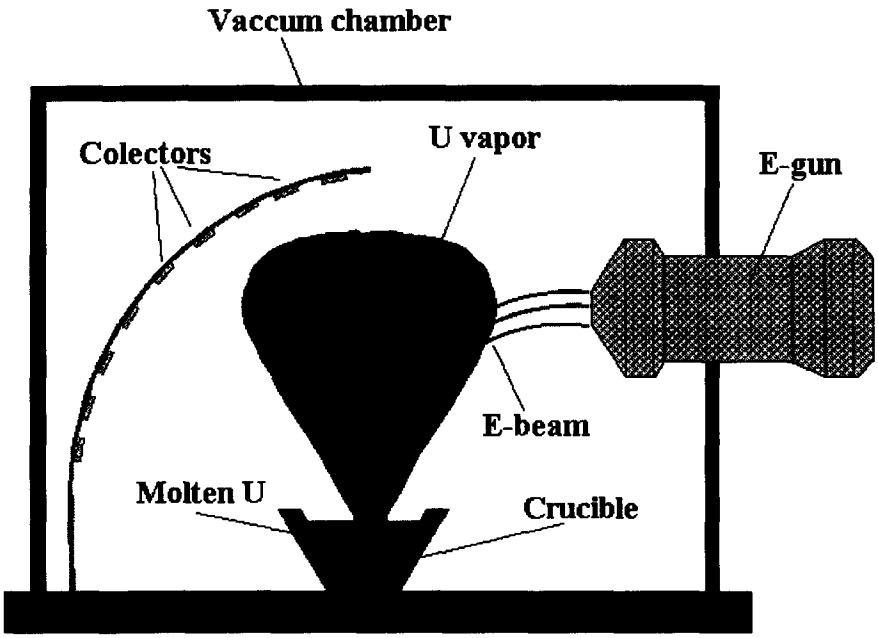

Fig. 31 - Experimental setup for uranium evaporation experiments.

Using the same vacuum chamber and e-beam, we are also running experiments to test thermal resistance and the resistance to chemical attack from liquid uranium for different materials.

Test crucibles are made departing from powder (oxides, carbides, nitrides etc.), filled with solid uranium and submitted to e-beam heating for many different temperatures and temperature variation rates. The crucible mechanical integrity is examined to verify cracks and snaps and, after being cut in pieces, the chemical attack is evaluated. The next step is to install a mass spectrometer to the system to evaluate the contamination each material (or set of materials) generates.

Another important aspect related to vapor handling is the collection of the enriched and depleted materials. Not only technological aspects must be considered but also some basic physical problems, with interdependent solutions, demand careful analysis. The first basic question is how to collect the photoionized uranium. For a directional beam composed by neutral atoms and ions, a pair of biased flat electrodes placed aside the vapor beam should be able to separate the ions. However, since the vapor beam is never perfectly collimated, a fraction of the vapor can migrate to the collectors, reducing the overall selectivity. Therefore, the geometry of the electrodes and their position with respect to the atomic beam is already a subject of study. Besides, the photoionization creates a cloud of ions and electrons that, depending on the charge density, can be characterized as a plasma (Chen, 1984). An electric field, for instance, applied to a plasma, tends to separate ions and electrons to opposite directions; as the opposite charges are separated, they generate an internal electric field that tends to cancel the external applied field. So, the plasma shields the applied field and the collection of charged particles is no more governed by the physics of simple charged particles in an electric field, and the ambipolar diffusion should be considered. The particles speed towards the collector plates can be considerably smaller than the free charges velocity. The solution for ions collection in AVLIS experiments usually considers collectors hidden by some convenient shutter, allied to crossed electric and magnetic fields, calculated to deviate the ions trajectory to the collectors. Nevertheless, crossed electric and magnetic fields, calculated for convenient orbits of ions, determine electron cyclotronic orbits with much smaller pitches than those for the ions due to the difference in mass; this can increase the number of collisions between electrons and neutrals, with possible ionizations that decrease the overall selectivity of the process. To summarize, the design of a system to collect photoions must consider geometry, plasma effects, electromagnetic fields configuration and so on. Fortunately, these are aspects that permit accurate modeling. The theoretical model mentioned above allows us to study these problems in two dimensions, having as boundary conditions the geometry of the electrodes and the magnitude of the applied fields and, as initial conditions, the neutral particles density and velocity distribution and the photoionization rate. The experimental setup to confirm the theoretical results is being assembled.

Supposing that the geometry and the method of ion collection are solved, there is still another interesting question: How do we remove both enriched and depleted collected materials, from the vacuum chamber in continuum operation? If one is studying the process, the experiment can be interrupted to replace the collectors. However, in a regular AVLIS process, a steady-state operation has to be considered. In this case a ribbon or a wire can be used, unrolling from a reel, passing by the collecting region and being rolled in another reel. Another solution is to keep collectors at a temperature high enough to keep the uranium in the liquid state (Baudrillart et al., 1996), so that, after condensing on the collector surface, it drops into special receptacles.

Certainly, the discussion presented here about uranium evaporation and collection just scratches the surface of the subject but, anyhow, the conclusion is that metal evaporation for AVLIS purposes is a multivariable problem and the trade off among these variables is a hard task to accomplish. We have prioritized the spectroscopy and the laser development aspects, however some studies about uranium evaporation have been performed. A numerical code to describe the plasma behavior and the collection mechanisms has been developed and a study of special refractory materials for crucibles resistant to uranium attack is being accomplished. The present effort is directed to the assembling of a new evaporator setup, foreseen to the begin of 1997. The new setup should allow deeper studies on uranium evaporation and collection, as well as on photoionization spectroscopy.

6. CONCLUSIONS

Uranium isotope enrichment is universally recognized as a very expensive activity. Its exercise is only justified by the necessity of energy generation by nuclear reactors. The laser methods for uranium enrichment are being considered, nowadays, among the best from the economical viewpoint. They are also widely regarded as the best ones from the ecological point of view, since the collected tails can be extremely depleted of the fissile isotope ^{235}U.

The use of laser methods for uranium isotope separation requires, on the other hand, an amount of scientific and technological knowledge which is not yet completely available. The involved problems comprise an interdisciplinary knowledge that no professional alone can dominate. Studies on basic science, technology, engineering and economics are necessary, which are beyond the academic formation of any conventional technician or scientist. Nevertheless, countries which possess already the traditional technologies in advanced stages make nowadays plans of giving up installations that are working, in favor of investments in these new techniques. In countries where the traditional technologies have not yet been deployed in a considerable scale, it seems reasonable that new investments be directed towards technologies that can offer the possibility of being competitive in near future in the international market.

The studies we have described in this paper are part of a project whose aim is to demonstrate the technical viability of the laser processes for isotope separation using, as long as possible, resources available in Brazil. It involves not only studying related processes but also the development of critical associated technologies. The main objectives of this work was to describe the laser processes for isotope separation and to present some useful results obtained in our laboratory. We focused our attention mainly on two actuation areas: laser development and spectroscopy. This paper presents some results obtained in these areas, such as CVL with average output power up to 40 W and the observation of three-photon, two-frequency photoionization of uranium both in hollow cathode lamps and in a furnace. Presently we are working towards the assembling of a new evaporation system and the new Cu-HBr lasers to the isotope separation setup. These new systems, besides helping the evaluation of the laser techniques of uranium enrichment, will allow better research in the area of multiphoton spectroscopy, that we have chosen as priority for our future research work.

ACKNOWLEDGMENTS

The authors wish to acknowledge all the colleagues of the IEAv who have given support to this research work We acknowledge also Dr. Lamartine F. Guimarães, from IEAv, for inviting the presentation of an invited paper at the 10th ENFIR and for encouraging us to write this paper. We thank also Prof. Ricardo C. de Barros, from the Universidade do Estado do Rio de Janeiro (UERJ) for the revision of the manuscript and for his clever comments on the use of the English spelling.

The research work we have described in this paper is being carried out under the auspices of the Secretary for Strategic Affairs (SAE) and the Ministry of Aeronautics of Brazil.

REFERENCES

Airoldi, V. J. T., C. C. Ghizoni, E. J. Corat, M. E. Sbampato and A. M. Santos (1988). Inhibition of formation of SF_6 molecular clusters in a free supersonic expansion. *J. Appl. Phys.*, 63, 5169-5171.

Ambartzumian, R. V. and V. S. Letokhov (1972). Selective Two-Step (STS) Photoionization of Atoms and Photodissociation of Molecules by Laser Radiation, *Appl. Opt.*, 11, n. 2, 354.

Anazawa, R. M., N. A. S. Rodrigues, R. Riva, K. K. Yum, A. L. Ribeiro, C. A. R .S. Wahlbuhl and C. Schwab (1994). Air cooled copper vapor laser, *RP/IEAv-029/94* (Internal Report in Portuguese).

Babin, F. and J. M. Gagné (1986). Characterization of an atom beam produced with the help of a hollow-cathode discharge. *Rev. Sci. Instrum.*, 57, 8, 1536-1541.

Barbieri, B., N. Beverini and A. Sasso (1990). Optogalvanic spectroscopy. *Reviews of Moderns Physics*, 12, 3, 603-644.

Baudrillart, R., M. Alexandre, G. Bordier and A. Rosengard (1996). Un exemple d'actinide dans tous ses états. *CLEFS CEA,* 31, 25-26.

Blaise, J. and L. J. Radziemski Jr (1976). Energy levels of neutral atomic uranium (U_I). *J. Opt. Soc. Am.*, 66, 7, 644-659.

Blumenfeld, L. and Soubbaramayer (1994). Power balance equation in electron beam evaporation process. In *Annals of the 4th Workshop on Separation Phenomena in Liquids and Gases*, 1-6 (Beijing, P.R. China, ed. Chuntong Ying).

Böhm, H. D. V. (1977). PhD Thesis, Hamburg Universität. *Report GKSS77/E/39.*

Böhm, H. D. V., W. Michaelis and C. Weitkamp (1978). Hyperfine structure and isotope shift measurements on ^{235}U and laser separation of uranium isotopes by two-step photoionization. *Opt. Commun.* 26, 2, 177-182.

Broglia, M., F. Catoni and P. Zampetti (1983). Optogalvanic detection of uranium high-lying levels. *Journal de Physique* C7, 11, 251-258.

Broglia, M., F. Catoni and P. Zampetti (1985). Simultaneous detection of optogalvanic and fluorescence signals in a hollow cathode lamp. *J. Opt. Soc. Am. B* 2, 4, 570-573.

Burke, J. J., D. A. Colling, A. E. Gorum and J. Creamspan (1976). *Physical Metallurgy of Uranium Alloys* (Brook Hill Publishing Co, Chestnut Hill, USA)

Carlson, L. R., J. A. Paisner, E. F. Worden, S. A. Johnson, C. A. May and R. W. Solarz (1976). Radiative lifetimes, absorption cross sections, and the observation of new high-lying odd levels of ^{238}U using multistep laser photoionization. *J. Opt. Soc. Am.*, 66, 8, 846-853.

Cavalcante, V. L. (1987). Enriquecimento isotópico de urânio, 2nd Ed. *Centro de Informaçoes Nucleares*, Rio de Janeiro, CIN/AI-006 (In Portuguese).

Chen, H. -L. and C. Borzileri (1981). Laser induced fluorescence studies of U_{II} produced by photoionization of uranium. *J. Chem. Phys.*,74, 11, 6063-6069.

Chen, F.F. (1984). *Introduction to Plasma Physics and Controlled Fusion* (Plenun Press, New York and London).

Corliss, C. H. and R. W. Bozman (1962). Experimental transition probabilities for spectral line of seventy elements, *US Natl. Bur. Stds.*, monograph N53 (US GPO, Washington, DC).

Corliss, C. H. (1976). Line strengths and lifetimes of levels in neutral uranium. *J. Res. NBS A*, 80, 1-7.

Corney, A. (1977). *Atomic and Laser Spectroscopy* (Clarendon Press – Oxford).

Coste, A, R. Avril, P. Blancard, J. Chatelet, D. Lambert, J. Legre, S. Liberman and J. Pinard (1982). New spectroscopic data on high-lying excited levels of atomic uranium. *J. Opt. Soc. Am.* 72, 1, 103-109.

Couairon, A. and Soubbaramayer (1992). Hydrodynamics of molten metals with convection-damping effects. In *Annals of the 3th Workshop on Separation Phenomena in Liquids and Gases*, 99-114 (Charlottesville, Virginia, USA, ed. Houston G. Wood).

Davis, J. I. and R. W. Davis (1977). Some Aspects of the Laser Isotope Separation Program at Lawrence Livermore Laboratory, *AIChE Symposium Series*, 73, n. 169, 69-75.

Davis, J. I., J. Z. Holtz and M. L. Spaeth (1982). Status and Prospects for Lasers in Isotope Separation, *Laser Focus* (Sep 1982), 49-54.

Demtröder, W. (1996). *Laser Spectroscopy, Basic Concepts and Instrumentation*, (2nd Enlarged Edition - Springer Verlag, Berlin).

Destro, M. G., C. C. Ghizoni and W. Lima (1991). Two photons absorption observation by optogalvanic detection in an uranium hollow cathode lamp. In *Annals of the Group of Optics, XIV Encontro Nacional de Física de Matéria Condensada (Nacional Meeting on Condensed Matter Physics)*, Caxambu, MG, May 7-11, Brazil (Ed. V. Bagnato and C. H. B. Cruz - in Portuguese).

Destro, M. G. and J. W. Neri (1992). Small-signal gain and saturation intensity in dye laser amplifiers. *Applied Optics* 31 , 33, 7007-7011.

Destro, M. G., C. Schwab, F. C. Cruz, A. Scalabrin, D. Pereira and A. Mirage (1992). Using intermodulated optogalvanic spectroscopy to measure isotope shifts and hyperfine structure at uranium. *Revista de Física Aplicada e Instrumentação - SBF* 7, 2, 64-70 (in Portuguese).

Destro, M. G. (1993). Uranium metal vapor laser spectroscopy. *PhD Thesis, CTA-ITA,* São José dos Campos (in Portuguese).

Dizard III, W. and M. Knapik (1994). USEC approves AVLIS commercialization; SWU Project to get $ 3-million monthly. *Nuclear Fuel,* 19, 15, 1-11.

Engleman Jr, R., R. A. Keller and C. A. Miller (1987). Effect of optical saturation on hyperfine intensities in optogalvanic spectroscopy. *J. Opt. Soc. Am. B* 2, 6, 897-902.

Erez, G., S. Lavi and E. Miron (1979). Simplified theory of the optogalvanic effect. *IEEE J. Quantum Electron.* QE-15, 2, 1328-1332.

Fuss, W. and K. L. Kompa (1981). The importance of spectroscopy for infrared multiphoton excitation. *Progress in Quantum Electronics* 7, 2, 117-151.

Gagné, J. M. M. Carleer, B. Leblanc, Y. Demers and B. Mongeau (1979a). Générateur de vapeur d'uranium: la lampe à cathode creuse pulsée. *Applied Optics* 18, 13, 2107-2111.

Gagné, J. M., B. Leblanc, B. Mongeau, M. Carleer et L. Bertrand (1979b) Étude par absorption d'un faisceau d'une vapeur d' ^{238}U ($^5L_6^o$) obtenue à l'aide d'une lampe à cathode creuse. *Applied Optics* 18, 7, 1084-1087.

Gerstenkorn, S., P. Luc, CI. Bauche-Arnoult et D. Merle (1973). Structure hyperfine du niveau fondamental, moments dipolaire et quadrupolaire de l'isotope 235 de l'uranium. *Le Journal de Physique* 34, 805-812.

Greenland, P. T. (1990). Laser isotope separation. *Contemporary Physics* 31, 6, 405-423.

Grossman, M. W.and T.A. Shepp (1991). Plasma Isotope Separation Methods. *IEEE Transaction on Plasma Science*, 19, 6, 1114-1122.

Hao-Lin Chen and C. Borzileri (1981). Laser induced fluorescence of U_{II} produced by photoionization of uranium. *J. Chem. Phys.* 74, 11, 6063-6069.

Harrington, C. D. and A. E. Ruehle (1959). *Uranium Production Technology* (D. Van Nostrand Company, Inc, Toronto, London, New York).

Janes, G. S., I. Itzkan, C. T. Pike, R. H. Levy and L. Levin (1976). Two-photon laser isotope separation of atomic uranium: spectroscopy studies, excited-state lifetimes, and photoionization cross sections. *IEEE J. of Quantum Electron.* QE-12, 2, 111-120.

Jensen, R. J., O'D. P. Judd and A. Sullivan (1982). Separating isotopes with lasers. *Los Alamos Science* 3, 1, 2-33.

Jones, D. R., A. Akerboom, A. Maitland and C. Little (1993a). Copper HyBrID laser producing 149 W at 2.4% efficiency and 112 W at 3.1% efficiency, *CLEO'93*, paper CThN8, 460-461.

Jones, D. R., A. Maitland and C. E. Little (1993b). A copper HyBrID laser of 120 W average output and 2.2% efficiency. *Opt. Quantum Electr.* 25, 261-269.

Kim, J. J. (1991). Metal vapor laser: a review of recent progress. *Opt. Quantum Electr.*, 23, S464-S476.

Knoeles, M. R. H., R. Foster-Turner and A. J. Kearsley (1994). Copper lasers go for industrial gold. *IEEE Circuits and Devices Magazine,* 10, 5, 39-42.

Kushner, M. J. (1981). A self-consistent model for high repetition rate copper vapor lasers. *IEEE J. Quantum Electr.*, QE-17, 9, 1555-1565.

Lago, A., G. Woehl and R. Riva (1989). A pulsed dye laser with grazing incidence and folded cavity. *Appl. Phys B* 49, 73-76.

Lawler, E., A. I. Ferguson, J. E. M. Glodsmith, D. J. Jackson and A. L. Schawlow (1979) Doppler-free intermodulated optogalvanic spectroscopy. *Phys. Rev. Letters* 42, 16, 1046-1049.

Lewis, K. D. (1993). Validation of criticality safety calculational methods for U-AVLIS plant project. *American Nuclear Society Meeting (Nashville, TN, 19-23 Sep. 1993)* Availability: INIS; Available from OSTI as DE93018590; NTIS; INIS; US Govt. Printing Office Dep.

Maniscalco, J. (1976). Systems studies, *Lawrence Livermore Laser Program Annual Report - 1975*, UCRL-50021-75, 17-56.

Miron, E., R. David, G. Erez, S. Lavi and L. A. Levin (1979). Laser spectroscopy of U_I using stepwise excitation and fluorescence detection. *J. Opt. Soc. Am.*, 69, 2, 256-264.

Neri, J. W., C. A. B. Silveira, N. A. S. Rodrigues, C. Schwab, R. Riva, M. G. Destro and A. Mirage (1996). Metal photoionization in the afterglow of a hollow cathode lamp (submitted to *J. Physics B*).

Neri, J. W., M. G. Destro, N. A. S. Rodrigues, C. Schwab, A. Mirage and L. Fucheng (1995). Uranium $^7M_7$ level lifetime measurements by two photons optogalvanic spectroscopy, *Proceedings of the Optics Group, XVIII National Meeting on Condensed Matter Physics* - Brazilian Physical Society (SBF), 305-308 (Ed. A. S. G. Neto - in Portuguese).

Rodrigues, N. A. S, C. Schwab, M. G. Destro, R. Riva and A. Mirage (1994). Highlights on the AVLIS program at IEAv/CTA. In *Annals of the 4th Workshop on Separation Phenomena in Liquids and Gases,* 31-40 (Beijing, P.R. China, ed. Chuntong Ying).

Sbampato, M. E. (1994). Characterization of UF_6 expansion in supersonic molecular beam by infrared spectroscopy. *PhD Thesis, USP- Instituto de Química* (in Portuguese).

Schäfer, F. P. (1973). Dye lasers. In *Topics in Applied Physics*, 1 (ed. F. P. Schäfer, Springer-Verlag, Berlin).

Schiller, S., U. Heisig and S. Panzer (1982). Electron Beam Technology (John Wiley & Son, New York, Chichester, Brisbane, Toronto, Singapore).

Schneider, K. R. (1994). LIS: the view from Urenco, *Proc. Of the 6th International Symposium on Advanced Nuclear Technology Research - Innovative Laser Technologies in Nuclear Energy*, 280-297.

Schwab, C. (1995). Separação de Isótopos por Laser: O Experimento do IEAv. 10th Meeting on Reactor Physics and Thermal Hydraulics (ENFIR), Águas de Lindóia, SP, Brazil, 7-11 Aug. 1995. Invited Paper.

Schwab, C, R. Riva, N .A. S. Rodrigues, R. M. Anazawa, C. P. Cobra, K. K. Yum, C. A. R. S. Wahlbuhl, M. G. Destro, A. L. Ribeiro, L. A. S. Toledo, A. Scalabrim and J. Watanuki (1991). Metallic vapor laser technology transference, *RP/IEAv*-001-R/91 (Internal Report in Portuguese).

Sewell, P.G. (1992). Restructuring of the Departament of Energy's Enrichment Program, *Fuel Cycle '90 Conference*, Nashville, TN (United States), 25-28 Mar 1990. *23038554* SONAR - INIS, Vol-23 Num-13 15/10/92.

Shuker, R., A Ben-Amar and G. Erez (1983). Theoretical and experimental study of the resonant optogalvanic effect in neon discharges. *J. de Physique*, C7, 35-45.

Siegman, A. E. (1986). *Lasers* (University Science Books Ed., Mill Valley, Ca).

Solarz, R. W., C.A. May, L. R. Carlson, E. F. Worden, S. A. Johnson and J. A. Paisner (1976). Detection of rydberg states in atomic uranium using time-resolved stepwise laser photoionization. *Phys. Rev. A* 14, 3, 1129-1136.

Sorem, M. S. and A. L. Schawlow (1972). Saturation spectroscopy in molecular iodine by intermodulated fluorescence. *Optics Comm.* 5, 3, 148-151.

Soubbaramayer (1987). Physical aspect of the isotope separation by laser induced selective ionization, with emphasis on model analysis, *Workshop on Separation Phenomena in Liquids and Gases*, 1, 28-152, (Darmstadt, 20–25 July 1987, West Germany).

Svelto, O. (1989). *Principles of Lasers* (Plenium Press, New York and London, Third Edition).

Wilkinson, W. D. (1962). *Uranium Metallurgy* 1 (Interscience Publishers, New York, London).